ONE DIMENSIONAL METALLO DIELECTRIC PHOTONIC CRYSTAL

by

Adalberto Alejo-Molina

M. Sc. major in Optics, INAOE

A Dissertation submitted in partial fulfillment of the requirements for the degree of:

DOCTOR OF SCIENCE

Major in OPTICS

at the

National Institute for Astrophysics, Optics and Electronics

July, 2010

Tonantzintla, Puebla

Advisor:

Dr. José Javier Sánchez-Mondragón

Optics Department

INAOE

[In the beginning...]

"Chen ta yaan ma' tu péek yeetel ch'een le éek'joch'e'enil, le alkab."

Popol Vuh

("There were only immobility and silence in the darkness, in the night.")

ABSTRACT

This dissertation is devoted to the study of photonic crystals in one dimension. The structure under analysis is a ternary stack dielectric-dielectric-metal and here it is named Metallo-Dielectric Photonic Crystal (MDPC). A brief review of the pure Dielectric Photonic Crystal (DPC) is given for establishing a context and comparing the results of this research. The quarter-wave stack is the core of all the discussion along the manuscript and the key equivalent analytical expressions are derived for the MDPC, such as the dispersion relation, maximum absorption, band diagrams and band gap width, in the case of normal incidence. Also, for the MDPC the region of validity of the band structure is defined comparing it with the transmittance. Then, some of these results are extended for the condition of oblique incidence, calculating formulas for the transversal electric and magnetic modes. The transfer matrix methodology was used in all the investigation.

RESUMEN

Esta tesis está dedicada al estudio de cristales fotónicos en una dimensión. La estructura bajo análisis es un "stack" ternario dieléctrico-dieléctrico-metal y en este trabajo es nombrado Cristal Fotónico Metalo-Dieléctrico (MDPC, por su siglas en inglés). Un breve resumen del Cristal Fotónico Dieléctrico (DPC, por sus siglas en inglés) es dado con el fin de establecer un contexto y poder comparar los resultados de esta investigación. El "stack" de cuarto de longitud de onda es el núcleo de toda la discusión presentada a lo largo de este manuscrito y las expresiones clave equivalentes analíticas han sido derivadas para el MDPC, tales como la relación de dispersión, la absorción máxima, el diagrama de bandas y el ancho del band gap, en el caso de incidencia normal. Además, para el MDPC la región de validez de la estructura de bandas ha sido establecida comparándola con la transmitancia. Posteriormente, algunos de estos resultados son extendidos para la condición de incidencia oblicua, calculando fórmulas para los modos trasversal eléctrico y magnético. El método de matriz de transferencia es utilizado en toda la investigación.

PREFACE

Periodicity plays a very important role in the universe and in particular in our world. Dimension and order have a major role in a variety of phenomena that can be seen in the nature. For example, beautiful colors in the feathers of some birds or the wings in butterflies are due to the microscopic ordering of their surfaces. Another case is the composed eyes of some insects and crustacean which allow to them sense the polarization of light.

The order, and other factors, of the atoms or molecules that form different substances define fundamental macroscopic features such as hardness, conductivity, refraction index and so on. A specific case where this happens is in the carbon atoms, when they are in an amorphous phase they are graphite but when they are in a particular order they made diamond. The first one is useless in high-tech applications and the second one can be used inclusive as an active material for lasing.

Superconductivity is another circumstance which illustrates our point. In this situation crystallinity, in combination with extremely low temperatures, allows the propagation of electrons with almost not scattering in the material avoiding in this manner losses for heating, i. e., there is not resistance in the material to the flux of current.

Then, different behavior is obtained in some situations depending on the presence or absence of periodicity. For electromagnetic radiation, and in particular light, it is well-known that when it propagates in some solid state crystals birefringence occurs. What happens then with the propagation of electromagnetic radiation in a periodic medium, if it is possible to design a crystal with specific dimensions and refraction indices? Some interesting behavior is presented by light propagating in such structures in some sense analogue with the behavior of electrons propagating in solid state crystals. In this case the periodic structures are made of dielectric materials and their dimensions are typically in nanometers or micrometers, they were named Photonic Crystals.

Photonic crystals are periodic artificial structures designed to control light, guiding and bending it. A crystal is a theoretical concept, it is defined as a periodic medium of infinite extension that fills all the space. Of course, in reality photonic crystals have defined sizes but they shared almost all the features with the theoretical ones. These properties make possible the design and construction of optical devices.

Nowadays the basic and common features and all possible Brave lattices of the photonics crystals are well-known and understood. However, the engineering of the photonic band gaps, the materials themselves and the combination of dielectric and metallic components in the photonic crystals are an active field of research and development of new devices and technologies.

This dissertation is devoted to photonic crystals in one dimension with at least one material with refraction index depending on the frequency. In the present case, the material with a refraction index as a function of frequency is modeled following Drude model and also takes account of the absorption. This means that our material is a metal. Therefore, the problem of calculate dispersion relation and band structure is more complicated by traditional procedures, as is discussed along the manuscript.

Chapter one of this dissertation is an introduction that explains the basic concepts on photonic crystals and background of the research, situating the context and importance of the work.

Next chapter starts with a review of the known features in one dimensional dielectric photonic crystals under the propagation of an electromagnetic wave for normal incidence. Two different approaches, transmittance and band diagrams, are compared and their coincidences and discrepancies pointed out. Then, the introduction of metal in the crystal is discussed for just two materials. As mentioned above, Drude model is used to describe the refraction index of the metal considering absorption. Finally, we analyze a ternary structure dielectric-dielectric-metal and our original results are presented.

The third chapter is an extension of the results found in chapter two but now we considered oblique incidence. This condition generates two possible states of polarization: transversal electric and transversal magnetic modes. Again, the dispersion relation is calculated for both modes and omnidirectional band gaps are found. Our results suggest the possibility of plasmon polariton propagation in the case of transversal magnetic mode.

As final chapter the conclusions of this work are exposed. Also, a future research direction is suggested and the principal steps and how to deal with the problem are outlined. Finally, an appendix is included with a detailed development of the transfer matrix methodology.

ACKNOWLEDGMENTS

I want to thank Prof. Jose Javier Sanchez Mondragon for his advice and support during all the time that took to me to finish the Ph. D.

Also, I acknowledgment to Drs.: Margarita Tecpoyotl Torres, Francisco Javier Renero Carrillo, Miguel Angel Basurto Pensado, Daniel Alberto May Arrioja, and J. Jesus Escobedo Alatorre. For their comments and suggestions that help me to improve this dissertation.

Thanks to the professors, administrative staff and other people that in some way taught me something or helped me in this research. In particular to the secretaries of the optics department and academic department: Patricia Sanpedro, Esther Montes, Rocío Rodas and Martha Olmos.

Lastly, I am grateful with the National Institute for Astrophysics, Optics and Electronics (INAOE) and the National Council for Science and Technology (CONACyT) for the scholarship number 183001 that they granted to me for doing my Ph. D.

DEDICATION

To my family and friends... All that matters in life!

CONTENTS

LIST OF FIGURES

CHAPTER ONE

INTRODUCTION TO PHOTONIC CRYSTALS

Fundamental concepts and definitions on photonic crystals, and related fields, are introduced in this chapter to benefit the lector unfamiliar with these topics and for the selfconsistency of the document. The origin and analogies that generated the term “Photonic Crystal” are explained and commented. Also, some applications and possible uses for photonic crystals are mentioned. Lastly, the organization of this work and general remarks of its content are given. In the same way the principal and original results for each chapter are briefly mentioned.

1.1 What is a Crystal?

A crystal is, in essence, a theoretical concept because it is defined as a periodic structure of fundamental building blocks that fills the whole space [1]. In Solid State Physics these fundamental blocks are atoms, groups of atoms or molecules whereas a Photonic Crystal (PC) is made of nanoscopic or mesoscopic structures depending on the design wavelength.

Any crystal can be described in terms of a lattice with a group of fundamental building blocks attached to each lattice point. These blocks are called “the basis” and their infinite repetition in the space form the crystal structure.

A lattice is a regular periodic arrangement of points in space. It is a mathematical abstraction. So, the crystal structure is formed only when a particular basis is attached identically to each lattice point, with every basis identical in composition, arrangement and orientation. An example of a crystal, a possible lattice and a possible basis to generate it, is sketched in Fig. 1.1. As the lector can see in the same figure, more than one lattice is always possible for a given structure. It is not feasible to select a basis until we have selected the lattice.

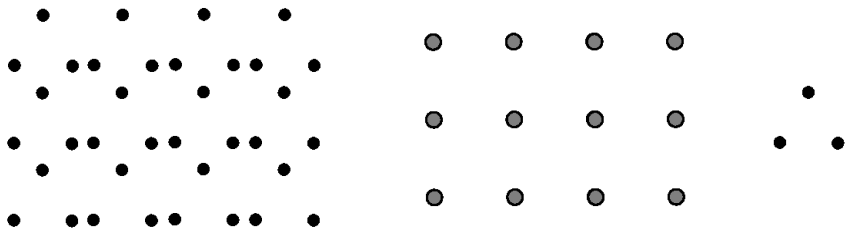

Fig. 1.1. The crystal, a possible lattice and one possible basis.

The lattice allows symmetry operations that carry the crystal structure into itself, like the lattice translation operation. Also, there are rotation and reflection operations. In some crystals it is possible to combine both types of operations. The symmetry operations for a particular crystal can be consulted in Ref. 1.

In one dimension (1D) there is only one possibility for a lattice and it is with all the lattice points on line. However, it is also possible to have any length between the lattice points. For the two dimensional case, the lattice has more freedom. In the same sense, that in the 1D, there is still an infinite number of lengths between two points of the lattice and also the angle between them does not have any natural restriction.

On the other hand, for a two dimensional (2D) space there are only five special types of lattices that allow symmetry operations. These special lattices are named Bravais lattices or two dimensional nets. This dissertation is limited to one dimension, but for completeness we would like to mention that in 3D there are fourteen Bravais lattices. An excellent introduction to crystallography can be consulted in Kittel's classic book [2] and in Ref. 3.

1.2 Why Photonic?

Electrons in atomic crystals interact with the ionic nucleuses which form the basis in some lattice. These electrons have still quantized states of energy and depending on the material result in defined energy bands.

Another form of explaining the energy band corresponds with the fact that electrons have wavelike behavior in a periodic medium and that the wavelength is defined by the De Broglie relation. This wavelength is on the order of the separation between the lattice points and their interference on the crystal atomic planes generates the energy bands and consequently the regions without propagation of electrons, i.e., energy band gaps.

Thus in atomic crystals the wavelike propagation of electrons into the crystal (periodic medium) generates energy band gaps. This is the case of an electromagnetic wave propagating in a periodic medium. This is the case of photonic crystals.

When a periodic medium is under the propagation of electromagnetic waves, the propagating "particles" are photons. The analogy between atomic crystal and dielectric crystals, as a periodic structure, is almost direct. The first case arises energy band gaps and the second one photonic band gaps. The last one owns its name to the quantization of the field of radiation, this means photons. Because, there are some regions where photons of specific

frequencies cannot propagate through the dielectric crystal and then the natural analogy is named photonic band gap and to the structure, photonic crystal.

Like atomic crystals, PCs can have defects of different types. However, in this case, defects can be controlled and engineered without difficulty at the will of the designer arising in this way photonic devices as technological applications that will be briefly commented in the following section.

1.3 Photonic Crystals: Importance and Technological Potential

It is almost impossible to start the study of photonic crystals without mentioning the pioneering work of Yablonovitch [4]. In that paper, he established the parallelism mentioned previously in this section. Therein, hundreds of papers and reviews have been written and new fields of research have appeared. However, that was the beginning of new composite material structures with new and special engineered properties based on its architecture.

Such is the case of the combination of PCs with thin metals that gave birth to Metallic-PCs [5]. A few years later, metamaterials started to become another important field of research with the fabrication and demonstration of the negative refractive index at a particular spectral range of frequencies [6]. Metamaterials are artificial periodic structures designed to have a strong response to the presence of electromagnetic fields. These special materials are composed of a mixture of different standard materials in a way that the effective index of refraction for a specific wavelength of design is negative (negative permittivity ε and permeability μ). Usually, the elements that constitute a metamaterial have smaller dimensions than the wavelength of

design and they have new electrical and magnetic features. They are also called negative index materials or left-handed materials.

The fundamental physical phenomena in those structures has demanded a growing attention. Such is the case of plasmons, a density of charge, coupled to an EM wave, which oscillates at optical frequencies in metallic/dielectric interfaces. MPCs and metamaterials are closely related to the current study of plasmon polariton devices. They started, a few years ago, combining periodic structures to enhance the plasmon's propagation [7].

All these topics are related trough the concept of periodicity but it is not just this feature, but the constructive interference of transmission and reflection and collective response. In addition, these kinds of nanostructures are capable of controlling light (electromagnetic radiation) in ways that previous devices were not. Thus, technological applications and expectations for optical devices based in these structures are high as a viable option to become a post-silicon technology.

In some applications, PCs devices have superior performance those traditional optical components. That is the case of PC filters with a very specific window of frequencies at the will of the designer. Another application is an optical splitter, dividing a waveguide into two. Also, with PC guiding, the light can be deviated to a right angle without theoretically leaking in contrast with the case of optical fibers where after some critical angle, light starts to escape. Mirrors with high reflectivity at a specific wavelength can be made essentially lossless. These mirrors can be used to generate cavities with a very high quality factor Q and their use in Cavity Quantum Electrodynamics is prominent. The fine details and some simulations of the devices described here can be consulted in Ref. 8 and 9 and references therein.

1.4 About This Manuscript

The present research is devoted to PCs in 1D in the presence of dissipative materials, in particular metals. The inclusion of metals in a composite of dielectric materials open new possibilities in the field of optoelectronic devices and often could be the substitutes of silicon technology because, in fact, many dielectrics used in PCs could be replaced by semiconductors.

There are four chapters altogether. The current one is a brief and general introduction to PCs, explaining the basic and fundamental concepts to their understanding and their technological implications. Nevertheless, each chapter has a short introduction to the particular case under discussion, resembling the state of the art and after that, original results which sustain this dissertation.

In the second chapter is discussed a ternary material ensemble with two different dielectrics and metal. Transmittance and band structure are calculated, analyzed and compared for the case of normal incidence.

Chapter three presents an extension of the methodology followed in the previous chapter, allowing in this manner the calculation of band structures for oblique incidence for both polarizations: Transversal electric and transversal magnetic modes. Omnidirectional band gaps are found due to the absorption in the metallic layers.

Finally, the conclusions of this work are presented and some remarks for future research on a two dimensional structure, which is a rare case where an analytical closed solution for the dispersion relation can be written using transfer matrix methodology in contrast to series-like with a lot of Fourier components resulting from the plane-wave method.

Also, an appendix with the Transfer Matrix Method is included at the end with the notation and modifications used along this manuscript. We strongly recommend to the reader unfamiliarized with the transfer matrix methodology to read appendix before the reading of chapter two. In the same way, perhaps, would be useful to read the basic concepts of crystallography discussed in chapters one and two from Ref. 2.

REFERENCES

[1]. T. Han (Editor). *International Tables for Crystallography, Volume A: Space Group Symmetry*, Springer, The Netherlands, 2005.

[2]. C. Kittel, *Introduction to Solid State Physics*, Wiley, New York, 1996.

[3]. N. W. Ashcroft and N. D. Mermin, *Solid State Physics*, Holt Saunders, Philadelphia, 1976.

[4]. E. Yablonovitch, Phys. Rev. Lett. **58**, 2059 (1987).

[5]. M. M. Sigalas, C. T. Chan, K. M. Ho and C. M. Soukoulis, Phys. Rev. B **52**, 744 (1995).

[6]. J. B. Pendry and D. R. Smith, Physics Today **57**, 37 (2004).

[7]. S. A. Maier, *Plasmonics: Fundamentals and Applications*, Springer, New York, 2007.

[8]. J. D. Joannopoulos, S. G. Johnson, J. N. Winn and R. D. Meade, *Photonic Crystals: Molding the Flow of Light*, Princeton University Press, Singapore, 2008.

[9]. K. Sakoda, *Optical Properties of Photonic Crystals*, Springer-Verlag, Berlin, 2005.

CHAPTER TWO

ONE DIMENSIONAL METALLO-DIELECTRIC PHOTONIC CRYSTAL NORMAL INCIDENCE

The difference besides a “pure” dielectric photonic crystal just called photonic crystal, one that contain metal and dielectric and finally a particular structure made of two different dielectrics and one metal is established on the context of this manuscript. Well-known facts are presented and discussed for the two first types of crystals mentioned before and compared with the original results found for the ternary material dielectric-dielectric-metal.

For this ternary material, that will be called metallo-dielectric photonic crystal, the dispersion relation is found analytically just in the case of normal incidence. Then the band structure is plotted and compared with the transmittance for validation. An enhancement effect is found in the transmittance, besides the presence of the metal, due to the existence of the periodicity and there is an increment in the band gap width. Also, new structural very thin band gaps appear due to the metal at frequencies beyond the plasma frequency. These band gaps are additional to the original ones of the basic photonic crystal and the ones of the metallic photonic crystal for low frequencies before the plasma frequency. Therefore both features coexist in the ternary structure that is proposed.

2.1 One Dimensional Dielectric Photonic Crystal

In essence a one dimensional dielectric photonic crystal (1D-DPC) is a stack made of two different dielectrics with, preferably, high contrast between their permittivity constants. A stack is a succession of parallel layers, with at least two different materials which alternate one after the other. The thickness of each layer in the stack could be constant or could follow a specific function.

Dielectric photonic crystals have been widely studied experimentally [1] since Second World War under the concept of thin-films. Thin-films are very important because their direct application in optical filters, antireflection films and coatings, but all their development was in some sense empiric knowledge of the materials and their combinations despite this kind of stratified media was first theoretical studied by Lord Rayleigh in 1887 [2].

General properties of periodic stratified media were investigated theoretically by Yeh and co-workers [3] setting the ground for the transfer matrix method (TMM) in Optics. The following results, for a stack dielectric-dielectric, are well-known in literature [4]. However, their inclusion here is essential to point out and to compare new results and contributions of this dissertation.

In Fig. 2.1 we show the dielectric-dielectric structure. It is constituted of two different dielectrics with indices n_1 and n_2, the thickness of each layer is a and b respectively. Then, the length of a unit cell is $L = a + b$, i.e., a period. A unit cell or primitive cell is a cell that fills all the space by the action of suitable crystal translation operations; a primitive cell is a minimum-volume cell.

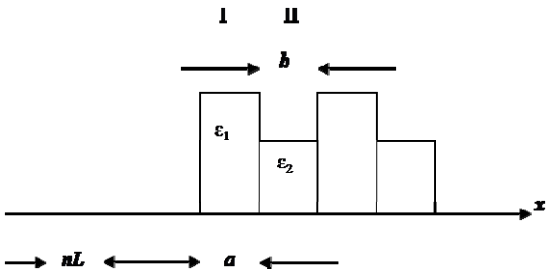

Fig. 2.1. Stack of two different dielectrics with indices n_1 and n_2.

The stack is engineered as a quarter-wave stack. Choose the λ/4 stack is not a fortuity one. This particular configuration of layered media is a special type named Bragg reflector because it exhibits resonance in the same way that the crystal lattice planes when are exposed to x-rays. Quarter-wave stacks are known for having high reflectance and the bigger stop gap in the transmittance curve. This occurs because the reflected waves for each layer are all exactly in phase at the midgap frequency [2]. A stop gap means a region in the transmittance where no frequencies are allowed to propagate through the structure.

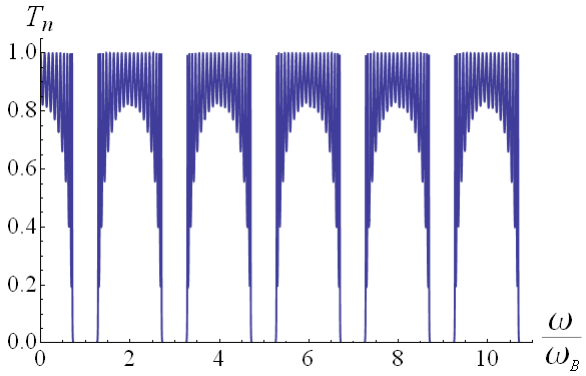

Fig. 2.2. Transmittance for a quarter-wave stack normalized to the design frequency.

A curve of transmittance for a quarter-wave stack, which only has ten unit cells, is shown in Fig. 2.2. For plotting this figure we use the Eq. (A22) and the following numerical values. The central wavelength has been chosen as λ_B = 1.55 μm (ω_B = 1.22 x 10^{15} rad/s), a telecommunication frequency, the thickness of each dielectric layer as $\lambda/4$ (due to the reason exposed before), i.e., a = 0.1082 μm, b = 0.2654 μm for the indices n_1 = 3.58 (Si) and n_2 = 1.46 (SiO_2), respectively. In this graph, we can appreciate the peculiarity that the first zero in transmittance (the stop gap) is centered at the wavelength of design (Bragg frequency) and the harmonics are exactly at two units of distance. Then, the stop gaps in this crystal are perfectly well-known.

Transmittance and reflectance are well-known concepts in Optics. However, in some particular topics, that are still considered branches of Optics, new concepts should be introduced, borrowed from other fields of Physics. Photonic crystals field is a good example of this need and a relative new concept that was adapted from Solid State Physics is band structure, as was exposed in chapter one. In the rest of this section, we will compare and discuss similarities and differences between transmittance and band structure.

Band structure is the plot of the dispersion relation. Roughly speaking, the dispersion relation establishes a mathematical function between the frequencies allowed in the crystal and special wave numbers that corresponds with those frequencies. These special wave numbers that can propagate trough the crystal are named Bloch wave numbers. Dispersion relation has only meaning for a crystal, this is, an infinity periodic medium.

Thus, using transfer matrix method, we derived the dispersion relation for the dielectric PC shown in Fig. 2.1. It is given by:

$$f(k_1,k_2)=\cos(\kappa L)=\cos(k_1a)\cos(k_2b)-\frac{k_1^2+k_2^2}{2k_1k_2}\sin(k_1a)\sin(k_2b), \qquad (2.1)$$

where κ is the Bloch wave number, the wave numbers k_i are defined in the usual way $k_i = (\omega/c)n_i$ $(i = 1, 2)$. The details of the Eq. (2.1) derivation can be consulted in the appendix.

Therefore, for this layered media, the band structure and the transmittance are shown in Fig. 2.3. For the numerical simulations we use the same numerical values that in the case of the transmittance in Fig. 2.2. In fact, to the right, we are reproducing again Fig. 2.2 but now it is rotated and the frequency axis rescaled at the same fashion that in photonic crystal literature and additionally it is normalized to the Bragg frequency ω_B. This means that we are using dimensionless variables in both axes.

On the other hand, in the left of Fig. 2.3, the band structure can be interpreted as follows. In the y axis there is a dimensionless frequency that is understood as the frequency which is illuminating the crystal whereas in the x axis the spatial frequency or wave number is plotted in the same way dimensionless. This wave number is the Bloch wave number and it is identified with the possible wave numbers that can be propagated through the crystal. Then, if a point in the x axis is chosen and it is possible to find a corresponding point in the frequency axis, this frequency can be propagated in the crystal with the Bloch wave number chosen before. In contrast, if it is not possible to find a frequency associated to one Bloch wave number, then, this frequency is not allowed in the crystal and will be reflected or will form a standing wave inside the crystal, not being transmitted to the other side of the material. These regions are named band gaps in the case of band structure diagrams and stop gaps in the case of transmittance graphs as can be seen in Fig. 2.3.

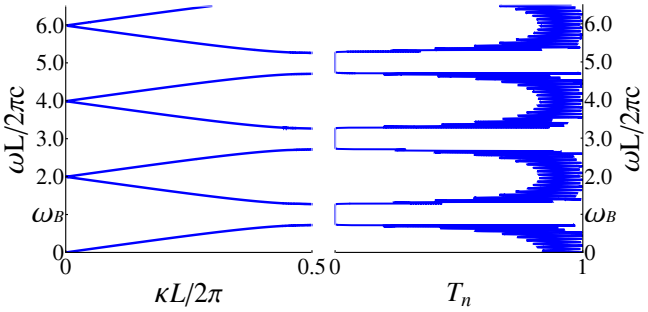

Fig. 2.3. Band structure and transmittance for the stack shown in Fig. 2.1.

We can appreciate from the above figure that the stop gap at the transmittance and the band gap in the band diagram match exactly in the case of dielectrics. A remarkable detail here is the fact that transmittance is just calculated for ten periods and the full stop gap is formed due to the high contrast between the dielectrics. In contrast, band structure is *ad infinitum* calculation.

Hence, we are comparing to different approaches that for one dimension proportionate, in some sense, the same information about the allowed frequencies in the crystal. However, transmittance is always valid and can be calculated for any specific number of layers and band structure is, in essence for an infinite crystal or semi-infinite crystal when superficial effects are considered. This will be a major difference when metal will be introduced in the structure as we will see in the next sections.

Mathematically, the band gaps are formed when the dispersion relation Eq. (2.1) takes values bigger than one. In that case, there are not solutions in the field of the real numbers for the dispersion relation and in the absence of absorption the band gaps just meaning frequencies not allowed in the crystal. However, when the band gaps are correlated with the transmittance we can see that the physical meaning is clearly a reflection of this range of frequencies. In contrast, stop gaps are just the zeros of the transmittance

function. Now, we will see what happened when metal is introduced in a photonic crystal and how the concept of band gap and absorption are modified by it.

2.2 One Dimensional Metallic Photonic Crystal

Often, a stack formed of a dielectric material and a metallic layer is called metallic photonic crystal (MPC) [5-10]. In all the works cited before, except one, for this kind of stack, metallic layers are thin (less than the skin depth) and the dielectric material is air (n_a = 1). One of the first works in MPC was due to Kuzmiak and Maradudin [5]. They presented two methods to deal with the metallic components in the case of 1D-DPC, the TMM model and perturbative plane-wave method (PWM). These authors calculated band structure for thin metallic layers in a regimen where band diagrams are still valid. In contrast, Yablonovitch and co-workers explored the opposite regimen of thick metallic layers where the inclusion of metal cannot be considered a perturbation and band structures are no longer valid. Therefore, in this section, we will discuss some features of the metallic photonic crystal described above and in the next one we will point out which of these features coexist in the structure that we are proposing and we will show that there is a particular dominion where band structure and transmittance are complemented.

As it is well-known, metals are highly dispersive and reflective in a wide range of frequencies, from microwave to far-infrared. Therefore, the penetration of electromagnetic waves into metals is negligible. But at higher frequencies towards the near-infrared and visible part of the spectrum, field penetration increases significantly and then dissipation too. In the range of ultra-violet frequencies, metals behave as dielectrics and allow the propagation of electromagnetic radiation. However there is still some degree

of attenuation, depending on the metal itself. In the case of noble metals, as gold or silver, there is strong absorption in this regime meanly due to transitions between electronic bands.

The dispersive properties can be described via a complex dielectric function $\varepsilon_m(\omega) = \varepsilon_R(\omega) + i\varepsilon_I(\omega)$. Thus, the index of the metal is given by $n_m = \varepsilon_m(\omega)^{1/2}$, and can be modeled through

$$\varepsilon_m(\omega) = 1 - \frac{\omega_p^2}{\omega(\omega + i\gamma)} \tag{2.2}$$

which is the Drude model with the following parameters: ω_p = 1.6 x 10^{16} rad/s (λ_p = 117.80 nm, UV) is the plasma frequency and γ = 0.001 ω_p is the damping coefficient, these are typical values for metals such as copper, gold, silver and aluminum. The model is in good agreement with alkali metals up to the ultraviolet and provides an acceptable description of the dielectric constant (index of refraction plus absorption) for noble metals, in a range of frequencies that includes low-frequency, radio waves and high-frequency, near-ultraviolet light.

Nevertheless, this model has problems when is compared to real values of noble metals [11] (such as gold and silver) in the visible due to the interband transitions for noble metals when $\omega > \omega_p$, then a correction is needed that basically consists in the substitution of the unit in Eq. (2.2) by an effective dielectric constant ε_∞ (usually $1 \leq \varepsilon_\infty \leq 10$) [12]. Additionally, it appears that below 20 nm it is difficult to grow a uniform film by evaporation and there are not bulk properties, which means that the dielectric constants are not independent of film thickness [11].

Moreover, in the case of composites, when the dimension of metallic components is on the order of few nanometers there are very interesting and unexpected phenomena such as nonlinearities. These nanoparticles can be modeled through and effective nonlinear refractive index [13] and via this

relation a new kind of soliton is found that in the limit case reduces to the Kerr soliton and in general is an amplitude oscillating soliton [14]. Further discussion about this nonlinearity and the new kind of soliton that it generates is beyond the scope of this dissertation and can be found in the reference cited before.

Now, returning to the discussion of the index for metals, their inclusion as layers in the structure implies losses which are the meaning of the damping coefficient γ in Eq. (2.2) and in optics, it is related directly with absorption as we will see after. For this binary stack the dispersion relation is the same that in Eq. (2.1) but with the appropriate changes. For DPCs, where all the components are non-absorbent dielectric materials, the Bloch wave number is a pure real number in the frequency range of transmission bands in the first Brillouin zone. However, in the band gaps the Bloch wave number is complex, with the real part in the limit of the Brillouin zone and the imaginary part varying as function of the frequency. Other circumstances with a complex Bloch wave number are modes allowed, due to defects, inside the range of frequencies in the band gap and surface modes.

In the MPC case there is a complex wave number for the metal with real (imaginary) part k_{2R} (k_{2I}) and the same happens for the Bloch wave number κ. That is κ is no longer a real number but a complex one:

$$\kappa = \kappa_R + i\kappa_I . \tag{2.3}$$

The real part of the Bloch wave number κ_R is associated with the index of refraction as well as the imaginary part κ_I is directly related to the absorption coefficient α as the inverse of the attenuation length according to the following definition:

$$\frac{1}{l} = \alpha = 2\kappa_I . \tag{2.4}$$

Thus Eq. (2.1), for this MPC, was solved by previous authors [5-9] numerically to determine a complex band structure, which, in addition the dispersion relation curves $\omega = \omega(k)$, also yield the absorption coefficient α of the corresponding mode. Band Structure and absorption are shown in Fig. 2.4 for a MPC with a = 0.1082 μm and b = 0.01 μm (metallic layer in this case).

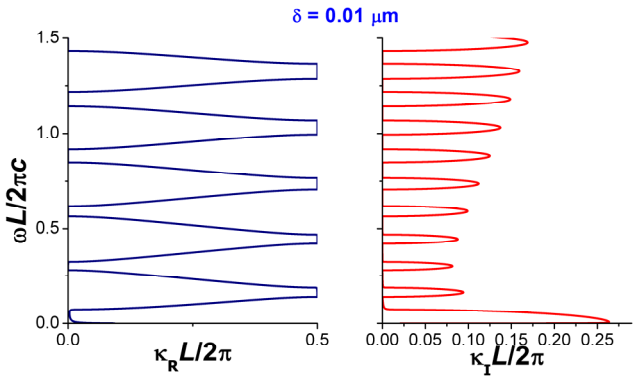

Fig. 2.4. Band structure and absorption for a metallic photonic crystal.

It is clear from Fig. 2.4 that there are band gaps for this particular combination of thickness and materials. The band gap at the bottom is mainly due to the absorption of the metal. There is a threshold frequency before which for low frequencies, almost all is absorbed. The other band gaps are structural band gaps, associated to the periodicity of the stack. It is interesting the fact that now there are band gaps at the beginning of the first Brillouin zone and not only at the end. However, there is also too much absorption in this structure and this band gaps are not periodic which made very difficult to describe them analytically.

A second approach, the PWM commonly used in PC topics, takes the calculation of the band structure to the generalized eigenvalue problem. It can be reduced to an equivalent set of nonlinear equations [5] which correspond to the diagonal terms of the matrix equation in the plane-wave representation.

However, it requires the diagonalization of a high-dimensional matrix of order 3*NG*, where *NG* is the number of plane waves used in the expansions, which makes the evaluation of the eigenvalues highly computer-intensive. The plane-wave approximation has problems for the additional modes below the lowest frequency band. Thus, we concluded that for this particular case of photonic crystal, the use transfer matrix method is the better approach for band diagrams calculation.

On the other hand, some experimental research has been done for this specific MPC (air and metal). Scalora and co-workers [7] have shown that the structure remains transparent even if the total amount of metal is increased to hundreds of skin depths in net thickness. This is, the concept of skin depth loses its meaning in the case of a periodic structure where the presence of spatial discontinuities of the index of refraction, alters the physical properties of the structure as a whole. Also, the coefficients of transmission and reflection could be engineered and the absorption is partially suppressed in the structure due to a coherent effect.

In the next section we will expose some of the key results of this dissertation for the case of a ternary structure composed of dielectric-dielectric-metal layers typically named metallo-dielectric photonic crystal (MDPC).

2.3 One Dimensional Metallo-Dielectric Photonic Crystal

The study of stacks could appear to be an old problem… but it is not! New effects and interesting phenomena [15] could be studied and modeled in this "well-known" structure, for example, combinations of positive and negative indices [16, 17], or linear with nonlinear and nonlinear-nonlinear stacks [18,19]. Also, new geometries, as for example Bragg fibers [20] or Bragg

onion [21, 22] can be explored beginning from the basic 1D-DPC. Only recently ternary systems in PCs have started to be studied in their different combinations. Stacks formed by three dielectrics were also anticipated by Yeh [3] and now engineering of the gaps [23] is a hot topic due to our actual technology and control of materials. In the case of 1D-MDPCs some work has been done before for a spherical shell onionlike in terms of transmittance [24].

The structure, that we proposed and investigated, is a 1D-MDPC formed of two dielectrics and metallic inserts. This is a ternary stack dielectric-dielectric-metal, i.e., a DPC is used as a substrate and the metallic layers inserted do not modify the periodicity but the length of period. The stack is shown in Fig. 2.5 and the index of refraction has the profile

$$n(x)=\begin{cases} n_1, & nL \le x < nL+a \\ n_2, & nL+a \le x < nL+a+b \\ n_3, & nL+a+b \le x < (n+1)L \end{cases} \tag{2.5}$$

as well as it satisfies the relation of periodicity

$$n(x)=n(x+L). \tag{2.6}$$

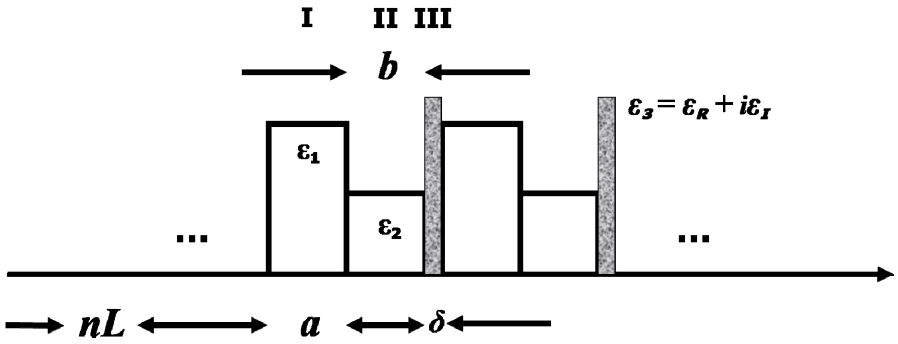

Fig. 2.5. Schematic representation of the MDPC stack.

The methodology followed to derive the dispersion relation and the transmittance of the system is the TMM. For the numerical simulations the same parameters that in section 2.1 are been used. As we said in the previous section, metal is modeled through Drude model and the thickness of the metallic layers will be changed as a parameter. First we will show some interesting phenomena found experimentally by Scalora [7] and after that commented by Yablonovitch [6], in both cases for metallic photonic crystal. In our case, Fig. 2.6 is presenting the transmittance for the metallo-dielectric photonic crystal. This transmittance is for different number of periods n, special attention should be taken to the enhancement in the transmission between two and ten periods in a finite stack, i.e., the structure has a total of thirty layers for ten periods. This plot corresponds to the case of 10 nm of thickness in each metallic layer, thus the total thickness of metal is 100 nm which in the case of silver with a central wavelength of 500 nm corresponds to a skin depth of approximately 10 nm. As was pointed before, this phenomena has its origin in a coherent feedback due to the periodicity of the structure and for the same reason to the discontinuities of the refraction index.

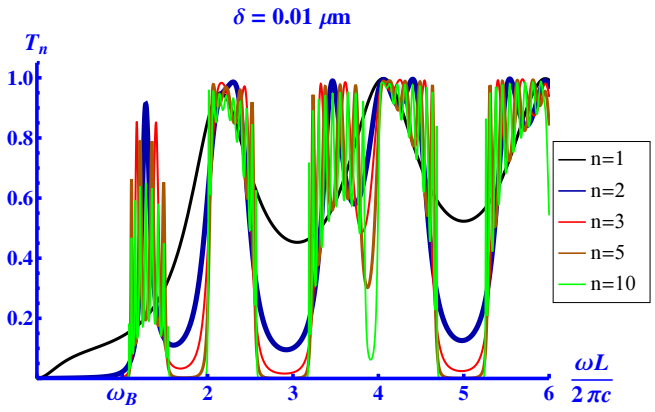

Fig. 2.6. The periodic metal array changes the concept of skin depth and partially suppresses the absorption as the field propagates within the material.

Also, it is notable the formation of an additional very thin stop gap in the neighborhood of $\omega L/2\pi c \sim 4$. These stops gaps are associated to the metallic layers but this will be discussed in detail in the sequence of graphs shown below.

Due to the high contrast between the indices of refraction in the dielectrics a full stop gap is formed before ten unit cells as can be appreciated in Fig. 2.7 (a), where there is not metal present and transmittance is shown for different number of periods. If we would like to take more unit cells the only variation in the stop gap will be faster oscillations and with less amplitude beside it.

The rest of the sequence in Fig. 2.7, not only shows the variation in the stop gap with respect to the number of periods but also shows how the change in the thickness of the metal, generates a full metallic stop gap which is thin at the beginning and gradually becomes thick. Furthermore, there is a shift in the central point of the stop gap and a broadening. The shift in the central point of the stop gap can be explained as a fundamental detuning, introduced in the resonance frequency due to the absorption or damping coefficient γ in Eq. (2.2). Further details can be consulted in Ref. 25. The broadening has its ground in the fact that the index of refraction of the metal is negative in a determinate range of frequencies and in this way, in average, the difference between the dielectric indices is larger. Then, as it is well-known, the larger the difference between the dielectric constants the bigger the stop gap and vice versa. It is interesting to mention that medium theories [26] cannot see the metallic stop gap as well as the effective index of refraction approach [27].

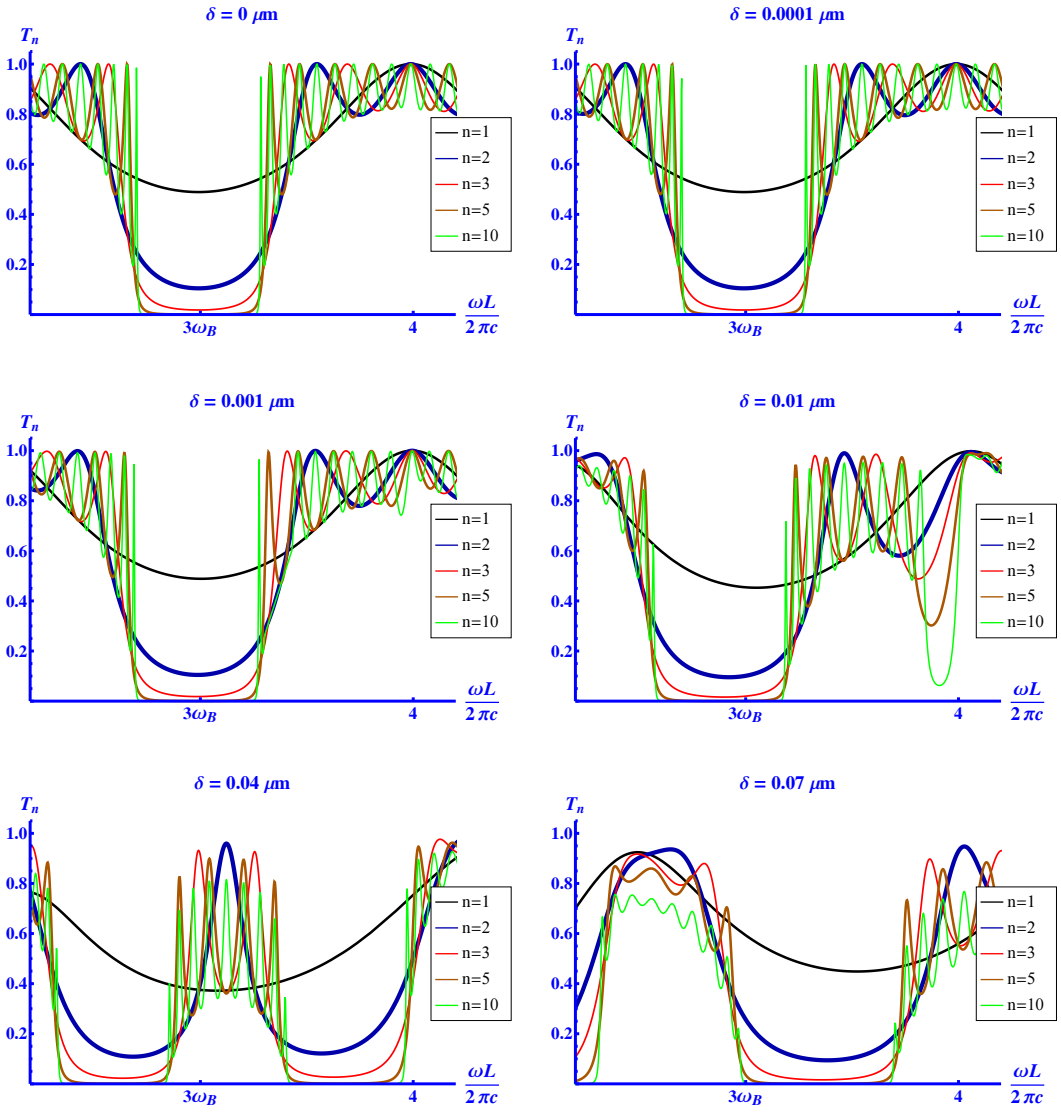

Fig. 2.7. Formation of a full stop gap with only ten primitive cells. The thickness of the dielectrics is fixed but in the metallic layers is changed: (a) $\delta = 0$, (b) $\delta = 0.0001$ μm, (c) $\delta = 0.001$ μm, (d) $\delta = 0.01$ μm, (e) $\delta = 0.04$ μm and (f) $\delta = 0.07$ μm.

Now the discussion about band structure will be continued for this kind of PC. In general, band structure is a calculation that implies an infinite periodic medium: a crystal. As was proved in the first section of this chapter, when there is not absorption, stop gaps in the transmittance coincide exactly with the band gaps in the band diagram. For semi-infinite or finite crystals band

diagrams suffer minor changes that are associated with the boundaries of the crystal generating superficial modes which could be engineering to the needs of the designer [2].

So, it is valid the band structure for a dissipative crystal? With this, there is an important implication, intuitively, if there is infinite or semi-infinite crystal with absorption at the end of the structure should not be anything transmitted. The answer is that this is true for a pulse but not for a continuum wave as will be seen later.

In contrast, transmittance is always valid, even in presence of absorption and can be calculated for any number of layers or unit cells. This can be strictly done also for the band structure for sufficiently large PC using FDTD techniques but it requires high computational resources. Thus transmittance will be used for validating the band diagrams.

Something that was not mentioned before is, that in the case of absorption in the PC there are two approaches. The first one corresponds to consider a complex frequency $\omega = \omega_R + i\omega_I$, where the complex frequency is associated with amplitude decaying in time and the Bloch vector is real and it extends infinitely in space. Conversely, the wave number is a complex quantity $\kappa = \kappa_R + i\kappa_I$, which in this case represents evanescent waves that decay as they propagate inside the crystal, whereas the frequency ω remains real. In general, one propagates an electromagnetic wave through the PC with a theoretical fixed real ω or a pulse with a determined spectral width. Thus, for this reason the second scheme was chosen.

Following the same methodology described in appendix (using TMM), just considering one more material, we derived the dispersion relation for normal incidence. Thus, the dispersion relation for the crystal shown in Fig. 2.5, is

$$\cos\left(\left[\kappa_R + i\kappa_I\right]L\right) = \left[\cos\left(k_1 a\right)\cos\left(k_2 b\right) - \frac{1}{2}\frac{k_1^2 + k_2^2}{k_1 k_2}\sin\left(k_1 a\right)\sin\left(k_2 b\right)\right]\cos\left(k_3 \delta\right) - \frac{1}{2k_3}\left[\frac{k_1^2 + k_3^2}{k_1}\sin\left(k_1 a\right)\cos\left(k_2 b\right) + \frac{k_2^2 + k_3^2}{k_2}\cos\left(k_1 a\right)\sin\left(k_2 b\right)\right]\sin\left(k_3 \delta\right) \tag{2.7}$$

where the wave number is defined in the usual way

$$k_i = \frac{\omega}{c} n_i \quad \left(i = 1, 2, 3\right). \tag{2.8}$$

Also, remember that $k_3 = k_{3R} + ik_{3I}$, because n_3 follows the Drude model. Dispersion relation, after some simple but cumbersome algebra can be expressed as two non-redundant [5] transcendental and coupled equations

$$\begin{aligned} p = \cos\left(\kappa_R L\right)\cosh\left(\kappa_I L\right) &= f\left(k_1, k_2\right)\cos\left(k_{3R}\delta\right)\cosh\left(k_{3I}\delta\right) \\ &- \frac{1}{2\left|k_3\right|^2}\alpha\left[k_{3R}\sin\left(k_{3R}\delta\right)\cosh\left(k_{3I}\delta\right) + k_{3I}\cos\left(k_{3R}\delta\right)\sinh\left(k_{3I}\delta\right)\right] \\ &- \frac{1}{2k_1 k_2}\beta\left[k_{3R}\sin\left(k_{3R}\delta\right)\cosh\left(k_{3I}\delta\right) - k_{3I}\cos\left(k_{3R}\delta\right)\sinh\left(k_{3I}\delta\right)\right]. \end{aligned} \tag{2.9}$$

This is the real part of the dispersion relation, whereas the imaginary part is given by

$$\begin{aligned} q = \sin\left(\kappa_R L\right)\sinh\left(\kappa_I L\right) &= f\left(k_1, k_2\right)\sin\left(k_{3R}\delta\right)\sinh\left(k_{3I}\delta\right) \\ &+ \frac{1}{2\left|k_3\right|^2}\alpha\left[k_{3R}\cos\left(k_{3R}\delta\right)\sinh\left(k_{3I}\delta\right) - k_{3I}\sin\left(k_{3R}\delta\right)\cosh\left(k_{3I}\delta\right)\right] \\ &+ \frac{1}{2k_1 k_2}\beta\left[k_{3R}\cos\left(k_{3R}\delta\right)\sinh\left(k_{3I}\delta\right) + k_{3I}\sin\left(k_{3R}\delta\right)\cosh\left(k_{3I}\delta\right)\right]. \end{aligned} \tag{2.10}$$

In equations (2.9) and (2.10), the function $f(k_1, k_2)$ is the original dispersion relation of the DPC substrate, Eq. (2.1). Other terms are introduced by the metallic layer and α and β are given by,

$$\alpha = k_1 \sin\left(k_1 a\right)\cos\left(k_2 b\right) + k_2 \cos\left(k_1 a\right)\sin\left(k_2 b\right), \tag{2.11}$$

$$\beta = k_2 \sin\left(k_1 a\right)\cos\left(k_2 b\right) + k_1 \cos\left(k_1 a\right)\sin\left(k_2 b\right). \tag{2.12}$$

The system of coupled transcendental equations (2.9) and (2.10), is typically solved numerically [28] but this procedure requires a high computational resource and shows some problems of convergence as we can appreciate in Fig. 2.8. This graph was obtained by using the computational procedure from Mathematica [29]. The explanation of this curve will be postponed until the introduction of our methodology to find the solutions of the system of equations that, to our best knowledge, is the first time that is proposed.

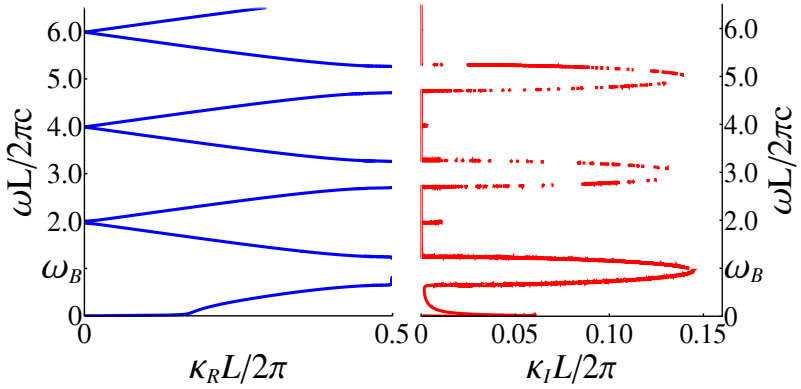

Fig. 2.8. Band structure and absorption, solving the system of equations for normal incidence and the thickness of each metallic layer is δ = 0.001 μm.

First, it is necessary to point out that p and q in Eqs. (2.9) and (2.10) are real for any physical parameters that can be evaluated. Then Eq. (2.7) can be expressed as follows

$$\cos\left(\left[\kappa_R + i\kappa_I\right]L\right) = p + iq. \tag{2.13}$$

Thus we can calculate the function *arccos* of a complex number by

$$\arccos w = \frac{\pi}{2} + i\ln\left(iw + \sqrt{1-w^2}\right), \qquad w = p + iq, \qquad p,q \in \mathbb{R} \tag{2.14}$$

which can be consulted in Ref. 30 but at there, it is incomplete and shifted with *arcsin* function. After some algebraic manipulation

$$\arccos w = \frac{\pi}{2} - \xi + \frac{i}{2}\ln\eta \tag{2.15}$$

where

$$\kappa_R = \frac{1}{L}\left(\frac{\pi}{2} - \xi\right) = \frac{\pi}{2L} - \frac{1}{L}\arctan\left(\frac{p + \left[\left(1+q^2-p^2\right)^2 + 4p^2q^2\right]^{1/4}\sin\frac{\theta}{2}}{-q + \left[\left(1+q^2-p^2\right)^2 + 4p^2q^2\right]^{1/4}\cos\frac{\theta}{2}}\right) \tag{2.16}$$

and

$$\kappa_I = \frac{1}{2L}\ln\eta = \frac{1}{2L}\ln\left(\left\{-q + \left[\left(1+q^2-p^2\right)^2 + 4p^2q^2\right]^{1/4}\cos\frac{\theta}{2}\right\}^2 + \left\{p + \left[\left(1+q^2-p^2\right)^2 + 4p^2q^2\right]^{1/4}\sin\frac{\theta}{2}\right\}^2\right) \tag{2.17}$$

the angle θ is calculated in the usual way

$$\theta = \arctan\left(\frac{-2pq}{1+q^2-p^2}\right). \tag{2.18}$$

After this, it is extremely easy to find the Bloch wave number just evaluating Eqs. (2.16) and (2.17) for different frequencies. Band structure of the MDPC under discussion will be shown and explained in the next figures.

In Fig. 2.9 is compared how the variations on thickness in the metallic layers modify absorption and the band structure and the last one is contrasted with the transmittance. It is necessary to say again that the band structure is *ad infinitum* calculation whereas the transmittance is only for ten unit cells and it is perfectly valid for these amounts of metal. So band structure reflex appropriately the behavior of the light in the crystal for thin metal layers as can be seen from Fig. 2.9 (a) to (c).

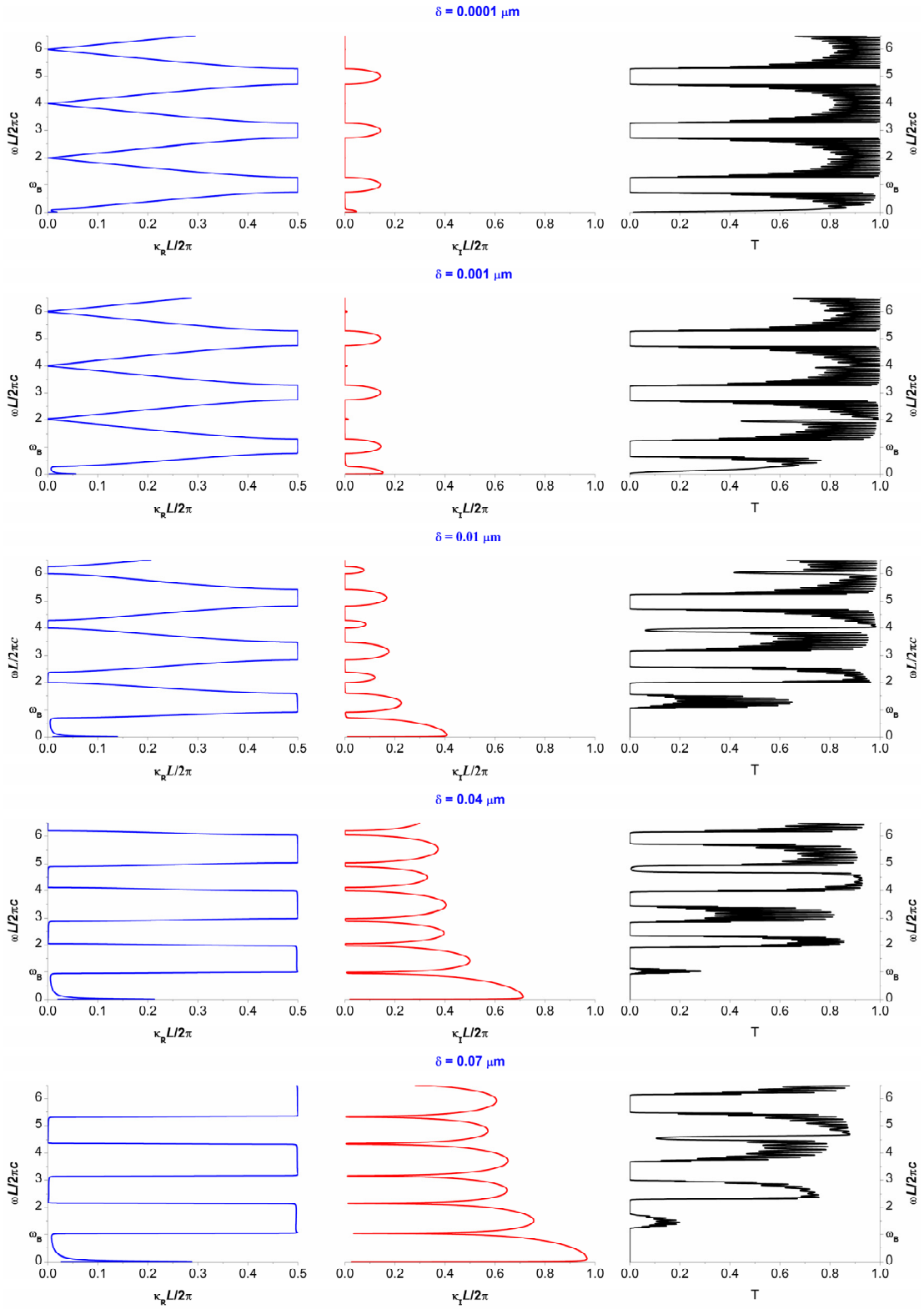

Fig. 2.9. Band structure, absorption and finally transmittance for different thickness of metal. (a) δ = 0.0001, (b) δ = 0.001, (c) δ = 0.01, (d) δ = 0.04 and (e) δ = 0.07 μm.

If Fig. 2.9 (a)-(d) is seen, it is appreciated in all the sequence a gradual change at the bottom of the first band, this is purely an effect of the absorption of the metal for low frequencies, i. e., before the plasma frequency all the frequencies will be attenuated or completely absorbed depending on the thickness of the metal; and after that, frequencies can propagate without problems.

Also, in the same figure the formation of a very narrow stop gap starts to appear between the dielectric stops gaps when the amount of metal is increased. This new stop gaps are clearly visible around 2.0 and 4.0 in the frequency axis of the transmittance (see Fig. 2.9 (b)). At the beginning these stops gaps are not visible in the band diagrams but when the metal thickness is 0.01 μm, we can see them also in the band diagrams as a band gap. Fig. 2.9 (c) shows a full band gap centered near 2.0, one more around 4.0 and another one close to 6.0 in the frequency axis. This means that the metallic layers generate an additional band gap between the usual structural band gaps originated by the DPC substrate, fact that is very remarkable because it is not predicted neither by medium theories [26] nor effective index of refraction approaches [27].

On the other hand, in Fig. 2.9 (d) and (e) there are no coincidence between the band gaps and the transmittance. As transmittance is completely valid for these amounts of metal, then band structures are no longer trusted and do not describe appropriately the behavior of the electromagnetic wave propagating in this medium. This is precisely the regimen where Ref. 6 is situated. The thickness of the metallic layers is big enough that cannot be considered a perturbation any longer.

However, in the transmittance we can appreciate the formation of full stop gaps and the fusion of the dielectric ones with the metallic ones originating a new stop gap wider than the original ones. Also, we can appreciate the

extinction of the low frequencies and the behavior reported by Yablonovitch and co-workers [6] for thick layers of metals in a MPC. The behavior that we are pointing out is the decay that the transmittance is suffering, adopting the form of isolated peaks that are no longer reaching the value of total transmittance.

Therefore, we showed the existence of metallic band gaps not only in the lowest band but also at high frequencies. These gaps are structural ones but different and additional to the dielectric ones in the DPC substrate as it was mention before. Moreover, comparing Fig. 2.8 with Fig. 2.9 (b) (reproduced together in Fig. 2.10), substantial differences can be seen due to the problem of solving numerically the equations and the need of techniques of convergence for the solutions which are not required using Eqs. (2.16) and (2.17). In the latter case the computational time is, for all purposes, negligible and the density of points can be increased as large as wanted.

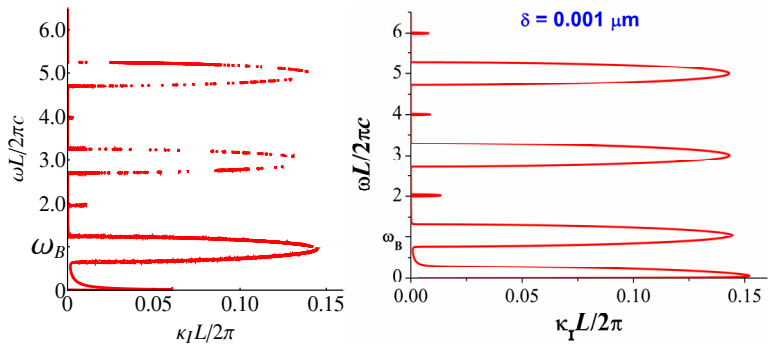

Fig. 2.10. Absorption, to the left solving the system of equations and right calculated through Eq. (2.17). Both graphics are for normal incidence (k_y = 0) and the thickness of the metallic layers δ = 0.001 μm.

Until now, we have been doing a phenomenological description of the band gaps and their localization. The next section will be focused in the development of analytical expressions which predict the position of the band gaps and estimate their widths.

2.4 Localization and Estimated Width of the Band Gaps

Our analytical description of the band gaps will be in terms of the dispersion relations and crystallographic concepts. However, we will also be doing reference to the transmittance graphs because in some cases it is easily to visualize a fact there.

This section will start with a very complete review of the methodology applied by Yeh [4] to estimate the width of the band gap and the approximate absorption in the band gap for a pure dielectric stack. After that we will extend this procedure to our ternary structure the MDPC and in this way predicts the approximated absorption and width of the dielectric and metallic band gaps which are formed in the MDPC.

For a 1D-DPC the band gaps are present when $k_1 a = k_2 b = \pi/2$, which is the $\lambda/4$ condition and according to our previous discussion this is happening for only a particular frequency, named Bragg frequency ω_B. Another fact is, in the band gap the absorption changes and has a maximum exactly at the center, this can be seen in Fig. 2.9 and in Fig. 2.10, we are going to represent the absorption with the letter "x". Now, the boundary of the Brillouin zone is located at $\mathrm{Re}\{\kappa\} = \pi / L$, thus

$$\kappa L = \pi \pm ix, \tag{2.19}$$

which means that the real part of the cosine function in the left part of Eq. (2.19) is close to 1 and the imaginary part x (absorption) will change along the band gap region, but in the boundaries will be cero. Therefore, at the frequency ω_B, condition (2.19) holds and the dispersion relation for two dielectrics Eq. (2.1), yields

$$x = \operatorname{arc\,cosh}\left(\frac{k_1^2 + k_2^2}{2k_1 k_2}\right). \tag{2.20}$$

Eq. (2.20) gives the maximum value for the absorption in the middle of the band gap. Nevertheless, the last expression can be manipulated to obtain an easily one, as follows. First, we will use the identity

$$\arccos f = \ln\left(f + \sqrt{f^2 - 1}\right) \qquad \left(f \geq 1\right) \tag{2.21}$$

where in our case f will be the argument of the inverse hyperbolic cosine function in Eq. (2.20). Then,

$$x = \left|\ln\left(\frac{k_1}{k_2}\right)\right| \tag{2.22}$$

and taking account of the expansion

$$\ln\zeta = \ln\left(\frac{1+g}{1-g}\right) \approx 2g + \ldots \tag{2.23}$$

where $g = \zeta - 1/\left(\zeta + 1\right)$ and also $\zeta = k_1 / k_2$, we finally arrive to

$$x = \operatorname{arc\,cosh}\left(\frac{k_1^2 + k_2^2}{2k_1k_2}\right) = \left|\ln\left(\frac{k_1}{k_2}\right)\right| \approx 2\frac{\left|k_1 - k_2\right|}{k_1 + k_2}. \tag{2.24}$$

This is the usual form in which it is found in the literature.

On the other hand, for calculating the approximate width of the band gap we will consider a small shift in the central frequency ω_B of the band gap, this shift will be named w, thus

$$k_1 a = k_2 b = \frac{\pi}{2} + w, \tag{2.25}$$

additionally, the band gap is in the border of the Brillouin zone and consequently it should satisfy condition (2.19), therefore the dispersion relation takes the form

$$\cos\left(\pi + ix\right) = \sin^2 w - \frac{k_1^2 + k_2^2}{2k_1k_2}\cos^2 w. \tag{2.26}$$

Simplifying the trigonometric functions:

$$w = \pm \arcsin\left(\frac{|k_1 - k_2|}{k_1 + k_2}\right) \approx \pm \frac{|k_1 - k_2|}{k_1 + k_2}. \tag{2.27}$$

However, w is a number and we need a frequency quantity. Our small displacement really means

$$k_{1B}a + \frac{\omega n_1 a}{c} = \frac{\omega_B n_1 a}{c} + \frac{\omega n_1 a}{c} = \frac{\pi}{2} + w, \tag{2.28}$$

and from the last equality

$$\omega = \frac{c}{n_1 a} w = \frac{\omega_B}{\frac{\omega_B n_1 a}{c}} w = \omega_B \frac{2}{\pi} w. \tag{2.29}$$

The combination of the last relation with Eq. (2.27) yields:

$$\omega_{\pm} = \pm \frac{2}{\pi} \frac{|k_1 - k_2|}{k_1 + k_2} \omega_B. \tag{2.30}$$

This omega has two signs because one defines the superior limit in the band gap and the other one the inferior value of it. Then, the total band width will be

$$\Delta\omega = \omega_+ - \omega_- = \omega_{\pm} = \frac{4}{\pi} \frac{|k_1 - k_2|}{k_1 + k_2} \omega_B. \tag{2.31}$$

Following this procedure we will apply an analogous one to calculate the maximum absorption for the 1D-MDPC and the width of the band gap. This can be done for both kinds of band gaps, the ones that appear in the odd harmonics (associated to the dielectric crystal) and in the same way the band gaps that correspond to the metallic layers in the even harmonics of the Bragg frequency.

The dispersion relation for the ternary structure is given by Eq. (2.7), also we will suppose that the metallic contribution to the phase will be small and condition $k_1 a = k_2 b = \pi/2$ is still valid.

To close this chapter we will proceed to describe the new type of band gap, found in this research due to the use of exact dispersion relations instead of medium theories.

The dielectric band gaps are formed when $k_1 a = k_2 b = \pi/2$ and between one harmonic and the next one there is a phase separation of 2π. Thus, as the metallic band gap is exactly at the middle of two dielectric ones, the condition should be modified to

$$k_1 a = k_2 b = \frac{\pi}{2} + \pi = \frac{3\pi}{2}, \tag{2.32}$$

because the half of 2π is π, plus the original phase of $\pi/2$ from the $\lambda/4$ condition. This condition is valid whenever the thickness of the metal δ is small.

Eq. (2.32) reduces the dispersion relation of the MDPC to:

$$\cos(\kappa L) = -\frac{1}{2}\frac{k_1^2 + k_2^2}{k_1 k_2}\cos(k_3 \delta). \tag{2.33}$$

In this case, the Eq. (2.19) still holds $\kappa L = \pi \pm i\kappa_I L,$ and therefore the dispersion relation changes to

$$\cos(\pi + i\kappa_I L) = -\frac{1}{2}\frac{k_1^2 + k_2^2}{k_1 k_2}\left[\cos(k_{3R}\delta)\cosh(k_{3I}\delta) - i\sin(k_{3R}\delta)\sinh(k_{3I}\delta)\right]. \tag{2.34}$$

Separating the last relation into real and imaginary parts, we arrive to the real part

$$\cosh(\kappa_I L) = \frac{1}{2}\frac{k_1^2 + k_2^2}{k_1 k_2}\cos(k_{3R}\delta)\cosh(k_{3I}\delta) \tag{2.35}$$

and the imaginary part is

$$\sin(k_{3R}\delta)\sinh(k_{3I}\delta) = 0 \tag{2.36}$$

From the imaginary part relation we find,

$$k_{3R}\delta = n\pi \quad (n \in \mathbb{N}), \tag{2.37}$$

this is because the hyperbolic sine function is only zero for $k_{3I}\delta = 0$. When this result is used in Eq. (2.35), yields

$$\cosh(\kappa_I L) = \frac{1}{2}\frac{k_1^2 + k_2^2}{k_1 k_2}\cos(n\pi)\cosh(k_{3I}\delta) \tag{2.38}$$

and so, we have an additional restriction for n, and it should be an even number because κ_I is defined positive according to our equations. With this new assumption we arrive to the solution

$$\kappa_I L = \operatorname{arccosh}\left(\frac{k_1^2 + k_2^2}{2k_1 k_2}\cosh(k_{3I}\delta)\right). \tag{2.39}$$

This represents the maximum absorption from the metal in the middle of the band gap. It is worth to mention that this expression is very similar to the one found before only for the dielectric crystal in Eq. (2.20), in our case we can see that there is a correction introduced for the metal and it depends directly to the thickness of the metallic sheet.

In analogy with the dielectric calculation, we will proceed to calculate the width of the metallic band gap. If a small shift to the low frequencies is considered on the neighborhood of the Bragg frequency for the metallic stop gaps, then

$$k_1 a = k_2 b = \frac{3\pi}{2} + y \tag{2.40}$$

and

$$k_{3R}\delta = 2n\pi + y \qquad (n \in \mathbb{N}). \tag{2.41}$$

Again evaluating this expression in the dispersion relation (2.7), also we should take account that we are working in the boundaries of the first Brillouin zone (κ_I = 0), thus it reduces to

$$\left[\sin^2 y-\frac{k_1^2+k_2^2}{2k_1k_2}\cos^2 y\right]\left[\cos y\cosh\left(k_{3I}\delta\right)-i\sin y\sinh\left(k_{3I}\delta\right)\right] \\ -\frac{1}{2k_3}\left[\frac{k_1^2+k_3^2}{k_1}\left(-\cos y\right)\sin y+\frac{k_2^2+k_3^2}{k_2}\sin y\left(-\cos y\right)\right]\left[\sin y\cosh\left(k_{3I}\delta\right)+i\sinh\left(k_{3I}\delta\right)\cos y\right]=-1. \tag{2.42}$$

After doing some cumbersome algebra, this expression can be separated in real and imaginary part. The real part is

$$\left[1-\frac{\left(k_1+k_2\right)^2}{2k_1k_2}\cos^2 y\right]\cos y\cosh\left(k_{3I}\delta\right)+\frac{k_{3R}}{2\left|k_3\right|^2}\left[\frac{k_1^2+\left|k_3\right|^2}{k_1}+\frac{k_2^2+\left|k_3\right|^2}{k_2}\right]\sin^2 y\cos y\cosh\left(k_{3I}\delta\right) \\ -\frac{k_{3I}}{2\left|k_3\right|^2}\left[\frac{\left|k_3\right|^2-k_1^2}{k_1}+\frac{\left|k_3\right|^2-k_2^2}{k_2}\right]\sin y\cos^2 y\sinh\left(k_{3I}\delta\right)=-1 \tag{2.43}$$

and the imaginary one yields

$$-\left[1-\frac{\left(k_1+k_2\right)^2}{2k_1k_2}\cos^2 y\right]\sin y\sinh\left(k_{3I}\delta\right)+\frac{k_{3R}}{2\left|k_3\right|^2}\left[\frac{k_1^2+\left|k_3\right|^2}{k_1}+\frac{k_2^2+\left|k_3\right|^2}{k_2}\right]\sin y\cos^2 y\sinh\left(k_{3I}\delta\right) \\ +\frac{k_{3I}}{2\left|k_3\right|^2}\left[\frac{\left|k_3\right|^2-k_1^2}{k_1}+\frac{\left|k_3\right|^2-k_2^2}{k_2}\right]\sin^2 y\cos y\cosh\left(k_{3I}\delta\right)=0 \tag{2.44}$$

Until this point we were working with exacts equations, in fact we can solve the last equations exactly but the solution will be very complicated and large. Therefore, we need to make an approximation to find an analytical solution not so cumbersome for y. Then, we are taking the expansions of the sine and cosine functions to order cero. For Eq. (2.44), this approximation results in

$$\left[\frac{\left(k_1+k_2\right)^2}{2k_1k_2}-1\right]\sinh\left(k_{3I}\delta\right)+\frac{k_{3R}}{2\left|k_3\right|^2}\left[\frac{k_1^2+\left|k_3\right|^2}{k_1}+\frac{k_2^2+\left|k_3\right|^2}{k_2}\right]\sinh\left(k_{3I}\delta\right) \\ +\frac{k_{3I}}{2\left|k_3\right|^2}\left[\frac{\left|k_3\right|^2-k_1^2}{k_1}+\frac{\left|k_3\right|^2-k_2^2}{k_2}\right]y\cosh\left(k_{3I}\delta\right)=0 \tag{2.45}$$

which can be immediately solved to

$$y=\frac{\left(n_1^2+n_2^2\right)\left|n_3\right|^2+n_{3R}\left(n_1n_2+\left|n_3\right|^2\right)\left(n_1+n_2\right)}{\left(n_1+n_2\right)\left(n_1n_2-\left|n_3\right|^2\right)n_{3I}}\tanh\left(k_{3I}\delta\right). \tag{2.46}$$

In this last step we only change $k_i \to n_i \quad (i = 1,2,3)$ in the fraction because all the constants will be canceled. Finally, the width of the metallic band gap will be

$$\Delta\omega_{Mgap} = \frac{4\omega_B}{3\pi} y. \tag{2.47}$$

This last relation is plotted in Fig. 2. 11 and compared with direct numerical measurements of the metallic band gap and also with the numerical fit, as can be seen the agreement is excellent.

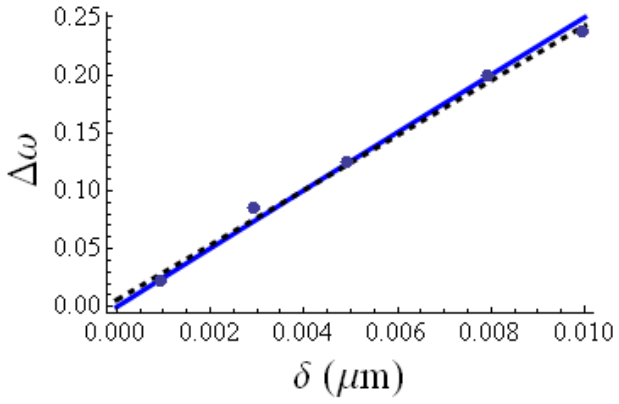

Fig. 2. 11. Solid line, the width of the metallic band gap described by Eq. (2.47). Circles are numerical measurements and dashed line is a numerical fit.

Summarizing, we demonstrated the existence of structural metallic band gaps in a ternary material, dielectric-dielectric-metallic, and we shown a manner to calculate it without the computational load that is usually required. Furthermore, the enhancement that is present in MPC is also presented in the MDPC that was studied, showing in this way that dielectric features and metallic ones coexist in this structure. In the next chapter this methodology will be extended to oblique incidence for transversal electric and transversal magnetic modes.

REFERENCES

[1]. H. A. Macleod, *Thin-Film Optical Filters*, Institute of Physics Publishing, Philadelphia, 2001.

[2]. J. D. Joannopoulos, S. G. Johnson, J. N. Winn and R. D. Meade, *Photonic Crystals: Molding the Flow of Light*, Princeton University Press, Singapore, 2008.

[3]. P. Yeh, A. Yariv and Ch. Hong, J. Opt. Soc. Am. **67**, 434 (1977).

[4]. P. Yeh, *Optical Waves in Layered Media*, Wiley & Sons, New Jersey, 2005.

[5]. V. Kuzmiak and A. A. Maradudin, Phys. Rev. B **55**, 7427 (1997).

[6]. H. Contopanagos, E. Yablonovitch and N. G. Alexopoulos, J. Opt. Soc. Am. A **16**, 2294 (1999).

[7]. M. Scalora, M. J. Bloemer, A. S. Pethel, J. P. Dowling, C. M. Bowden and A. S. Manka, J. Appl. Phys. **83**, 2377 (1998).

[8]. D. Soto-Puebla, M. Xiao and F. Ramos-Mendieta, Phys. Lett. A **326**, 273 (2004).

[9]. M. Bergmair, M. Huber and K. Hingerl, Appl. Phys. Lett. **89**, 081907-1 (2006).

[10]. M. Bergmair and K. Hingerl, J. Opt. A **9**, S339 (2007).

[11]. P. B. Johnson and R. W. Christy, Phys. Rev. B **6**, 4370 (1972).

[12]. S. A. Maier, *Plasmonics: Fundamentals and Applications*, Springer, New York, 2007.

[13]. K. Uchida, S. Kaneko, S. Omi, C. Hata, H. Tanji, Y. Asahara, A. J. Ikushima, T. Tokizaki and A. Nakamura, J. Opt. Soc. Am. B **11,** 1236 (1994).

[14]. J. J. Sánchez Mondragón, M. Torres Cisneros, E. Pérez-Careta, O. G. Ibarra-Manzano, O. S. Magaña Loaiza and C. Vázquez Ordoñez. Memorias en Extenso LII CONGRESO NACIONAL SMF/XXII REUNION ANUAL AMO, Acapulco, Guerrero, México, 2009.

[15]. G. Adamo, K. F. MacDonald, Y. H. Fu, C-M. Wang, D. P. Tsai, F. J. García de Abajo and N. I. Zheludev, Phys. Rev. Lett. **103**, 113901 (2009).

[16]. S. B. Cavalcanti, M. de Dios-Leyva, E. Reyes-Gómez and L. E. Oliveira, Phys. Rev. B **74**, 153102 (2006).

[17]. S. B. Cavalcanti, M. de Dios-Leyva, E. Reyes-Gómez and L. E. Oliveira, Phys. Rev. E **75**, 026607 (2007).

[18]. J. Escobedo-Alatorre, J. Sánchez-Mondragón, M. Torres-Cisneros, R. Selvas-Aguilar and M. Basurto-Pensado, Optical Materials **27**, 1260 (2005).

[19]. J. Escobedo-Alatorre, J. Sanchez-Mondragon, M. Tecpoyotl-Torres, G. Martinez-Nikonoff and E. Alvarado-Mendez, Proc. of SPIE **5184**, 156 (2003).

[20]. P. Yeh, A. Yariv and E. Marom. J. Opt. Soc. Am. **68**, 1196 (1978).

[21]. Y. Xu, W. Liang, A. Yariv, J. G. Fleming and S-Y. Lin. Opt. Lett. **28,** 2144 (2003).

[22]. A. Zamudio-Lara, J. Escobedo-Alatorre, J. Sánchez-Mondragón and M. Tecpoyotl-Torres, Optical Materials **27**, 1255 (2005).

[23]. S. K. Awashi and S. P. Ojha, Prog. Electromagn. Res. M **4**, 117 (2008).

[24]. A. Zamudio-Lara, J. J. Sánchez-Mondragón, M. Torres-Cisneros, J. J. Escobedo-Alatorre, C. Velásquez Ordóñez, M. A. Basurto-Pensado, L. A. Aguilera-Cortes, Optical Materials **29**, 60 (2006).

[25]. A. Alejo-Molina, *Decoherencia Semiclásica en Átomos de Dos Niveles y Puntos Cuánticos*. Tesis de Maestría. INAOE, 2006. (Unpublished)

[26]. A. A. Krokhin and P. Halevi, Phys. Rev. B **53**, 1205 (1996).

[27]. X. Xu, Y. Xi, D. Han, X. Liu, J. Zi and Z. Zhu, Appl. Phys. Lett. **86**, 091112 (2005).

[28]. A. Alejo-Molina, J. J. Sánchez-Mondragón, D. A. May-Arrioja, D. Romero, J. Escobedo-Alatorre and A. Zamudio-Lara, Microelectron. J. **40,** 459 (2009).

[29]. S. Wolfram, *Mathematica*, Addison-Wesley, Reading, MA, 1988.

[30]. G. Arfken, *Mathematical Methods for Physicists*, Academic Press, London, 1985.

CHAPTER THREE

ONE DIMENSIONAL METALLO-DIELECTRIC PHOTONIC CRYSTAL OBLIQUE INCIDENCE

All the results presented in this chapter, for the metallo-dielectric photonic crystal, are original and have not been published previously elsewhere. The chapter starts explaining the difference between normal and oblique incidence. Then, an extension of our methodology applied in the previous chapter is explained and developed. This procedure allows the calculation of the transversal electric and transversal magnetic modes in the structure under study. Lastly, band diagrams for both polarizations are presented and the existence of omnidirectional band gaps is pointed out. These band gaps depend in the thickness of the metallic layers and in the amount of absorption that wish to be allowed.

3.1 Oblique Incidence

In Geometric Optics, when a ray insides in a flat surface not perpendicular to it but with a tilt angle, it is named oblique incidence. In the case of Physical Optics, the wave vector makes the analogy with the ray and it is oblique incidence when the wave vector is not perpendicular to the surface.

In contrast, a mayor difference is that, Physical Optics takes account of the polarization of light whereas Geometrical Optics does not. Therefore in the former case there are two polarizations: transversal electric (TE) and transversal magnetic (TM) modes.

An *s* wave is another name given to the TE mode, it consists in a plane wave with the polarization of the electric field transversal to the plane of incidence. Of course for the TM mode, there is an equivalent in this terminology and it is known as *p* wave. This means that the polarization of the magnetic field is perpendicular to the plane of incidence, both polarizations are schematically shown in Fig. 3.1.

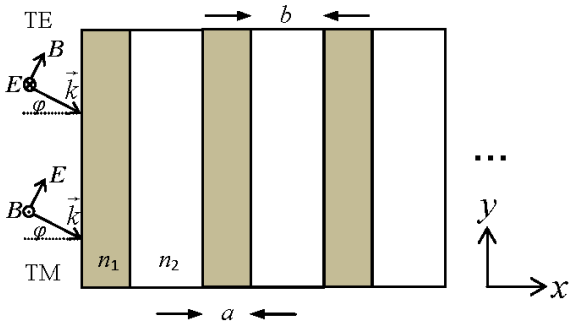

Fig. 3.1. Schematic representation of TE and TM polarizations in the crystal.

The analysis will be done for both, the TE and TM modes at the same time. Because traditionally it has been presented like that in the literature and the band diagrams are complemented if it is reflected through the vertical axis as would be seen in the next section.

3.2 TE and TM Modes of the One Dimensional Metallo-Dielectric Photonic Crystal

In the ternary structure that we proposed (Fig. 2.5), for oblique incidence is still applicably the TMM with the appropriate modifications, as will be shown below. First, as was explained in the previous section, will be two polarizations. For each polarization different modes can be propagated through the crystal depending on the angle of incidence which forms the wave vector with the normal to the crystal's surface.

There are two equivalent mechanisms to select the tilt, the first one is the angle of incidence and the second one, that will be used here, is considering the specific component in the k_y direction of the wave vector. This means that

$$k_{ix} = \sqrt{\left(\frac{\omega}{c} n_i\right)^2 - k_y^2}, \qquad (i = 1, 2, 3) \tag{3.1}$$

is changing over all possible values of k_{ix} (the subscript x will be drop in the following) when the component k_y is modified; and $n_i = \varepsilon_i^{1/2}$ (i = 1, 2, 3). Thus, the angle of incident will be modified indirectly through the component k_y. In fact k_y and the angle of incidence φ are related through the trigonometric relation $k_y = \left|\vec{k}\right| \sin\varphi$, which can be easily verified from Fig. 3.1.

A constrain is that k_i, in Eq. (3.1), must be a real number for the dielectrics. Eq. (3.1) is very important because allows us to calculated the TE and TM modes for every angle of incidence.

In the case of TE mode, the MDPC under study has the same dispersion relation, presented for the normal case in chapter two and deduced in the appendix. According to Eqs. (2.6) to (2.12), the dispersion relation is given by:

$$\cos\left(\left[\kappa_R + i\kappa_I\right] L\right) = p + iq \tag{3.2}$$

the real part is

$$\begin{aligned} p_E = {} & f_E\left(k_1,k_2\right)\cos\left(k_{3R}\delta\right)\cosh\left(k_{3I}\delta\right) \\ & -\frac{\alpha_E}{2}\left[k_{3R}\sin\left(k_{3R}\delta\right)\cosh\left(k_{3I}\delta\right)+k_{3I}\cos\left(k_{3R}\delta\right)\sinh\left(k_{3I}\delta\right)\right] \\ & -\frac{\beta_E}{2}\left[k_{3R}\sin\left(k_{3R}\delta\right)\cosh\left(k_{3I}\delta\right)-k_{3I}\cos\left(k_{3R}\delta\right)\sinh\left(k_{3I}\delta\right)\right] \end{aligned} \tag{3.3}$$

whereas the imaginary part is given by

$$\begin{aligned} q_E = {} & f_E\left(k_1,k_2\right)\sin\left(k_{3R}\delta\right)\sinh\left(k_{3I}\delta\right) \\ & +\frac{\alpha_E}{2}\left[k_{3R}\cos\left(k_{3R}\delta\right)\sinh\left(k_{3I}\delta\right)-k_{3I}\sin\left(k_{3R}\delta\right)\cosh\left(k_{3I}\delta\right)\right] \\ & +\frac{\beta_E}{2}\left[k_{3R}\cos\left(k_{3R}\delta\right)\sinh\left(k_{3I}\delta\right)+k_{3I}\sin\left(k_{3R}\delta\right)\cosh\left(k_{3I}\delta\right)\right]. \end{aligned} \tag{3.4}$$

We want to point out that both p and q are real. As before the wave vectors of the metal are complex numbers with real (imaginary) part k_{3R} (k_{3I}) and the same occurs for the Bloch wave vector κ_R (κ_I). In equations (3.3) and (3.4), the function $f_E(k_1, k_2)$ is the original dispersion relation of the DPC substrate, Eq. (2.1), reproduced again here for the comfort of the reader:

$$f_E\left(k_1,k_2\right)=\cos\left(k_1a\right)\cos\left(k_2b\right)-\frac{k_1^2+k_2^2}{2k_1k_2}\sin\left(k_1a\right)\sin\left(k_2b\right). \tag{3.5}$$

α_E and β_E in Eqs. (3.3) and (3.4) are defined as follows:

$$\alpha_E=\frac{k_1}{\left|k_3\right|^2}\sin\left(k_1a\right)\cos\left(k_2b\right)+\frac{k_2}{\left|k_3\right|^2}\cos\left(k_1a\right)\sin\left(k_2b\right) \tag{3.6}$$

and

$$\beta_E=\frac{1}{k_1}\sin\left(k_1a\right)\cos\left(k_2b\right)+\frac{1}{k_2}\cos\left(k_1a\right)\sin\left(k_2b\right). \tag{3.7}$$

In Eqs. (3.3) to (3.7) all the wave numbers k_i (i = 1, 2, 3) are given by Eq. (3.1) but it was not written explicitly for clarity in the expressions. The same should be understood for the TM case.

Following exactly the same reasoning that in the preceding chapter it is found that the real part of the Bloch wave vector is

$$\kappa_R = \frac{\pi}{2L} - \frac{1}{L}\arctan\left(\frac{p+\left[\left(1+q^2-p^2\right)^2+4p^2q^2\right]^{1/4}\sin\frac{\theta}{2}}{-q+\left[\left(1+q^2-p^2\right)^2+4p^2q^2\right]^{1/4}\cos\frac{\theta}{2}}\right) \tag{3.8}$$

and the imaginary part:

$$\kappa_I = \frac{1}{2L}\ln\left(\left\{-q+\left[\left(1+q^2-p^2\right)^2+4p^2q^2\right]^{1/4}\cos\frac{\theta}{2}\right\}^2+\left\{p+\left[\left(1+q^2-p^2\right)^2+4p^2q^2\right]^{1/4}\sin\frac{\theta}{2}\right\}^2\right), \tag{3.9}$$

where p and q are described according to Eqs. (3.3) and (3.4), respectively. As before,

$$\theta = \arctan\left(\frac{-2pq}{1+q^2-p^2}\right). \tag{3.10}$$

On the other hand, in the case of TM modes it is necessary to recalculate the transfer matrix from the beginning, because the boundary conditions in the Maxwell's equations are different and now the electric field is not analyzed but the magnetic one. This is the easy way and the dispersion relation is completely the same [1] that if it is calculated through the electric field. To calculate the dispersion relation for the TM mode using again the boundary conditions of the electric field implies to take account of the two components of this field. Therefore, the number of equations under analysis is duplicated.

Hence, this means that the TMM requires the H_z and E_y components in the place of E_z and H_y components from Appendix, respectively.

The dispersion relation for the TM modes has the same general form stated in Eq. (3.2), but in this case p and q have different definitions:

$$\begin{aligned} p_M = & f_M\left(k_1,k_2\right)\cos\left(k_{3R}\delta\right)\cosh\left(k_{3I}\delta\right) \\ & -\frac{\alpha_M}{2}\left(\varepsilon_I k_{3I}+\varepsilon_R k_{3R}\right)\sin\left(k_{3R}\delta\right)\cosh\left(k_{3I}\delta\right) \\ & +\frac{\beta_M}{2}\left(\varepsilon_I k_{3R}-\varepsilon_R k_{3I}\right)\sinh\left(k_{3I}\delta\right)\cos\left(k_{3R}\delta\right) \end{aligned} \tag{3.11}$$

and

$$\begin{aligned} q_M = & -f_M\left(k_1,k_2\right)\sin\left(k_{3R}\delta\right)\sinh\left(k_{3I}\delta\right) \\ & -\frac{\alpha_M}{2}\left(\varepsilon_I k_{3I}+\varepsilon_R k_{3R}\right)\sinh\left(k_{3I}\delta\right)\cos\left(k_{3R}\delta\right) \\ & -\frac{\beta_M}{2}\left(\varepsilon_I k_{3R}-\varepsilon_R k_{3I}\right)\sin\left(k_{3R}\delta\right)\cosh\left(k_{3I}\delta\right), \end{aligned} \tag{3.12}$$

where

$$f_M\left(k_1,k_2\right)=\cos\left(k_1 a\right)\cos\left(k_2 b\right)-\frac{\left(n_1^2 k_2\right)^2+\left(n_2^2 k_1\right)^2}{2\left(n_1 n_2\right)^2 k_1 k_2}\sin\left(k_1 a\right)\sin\left(k_2 b\right), \tag{3.13}$$

$$\alpha_M=\left(\frac{k_2}{n_2^2\left|k_3\right|^2}+\frac{n_2^2}{k_2\left|\varepsilon_3\right|^2}\right)\cos\left(k_1 a\right)\sin\left(k_2 b\right)+\left(\frac{k_1}{n_1^2\left|k_3\right|^2}+\frac{n_1^2}{k_1\left|\varepsilon_3\right|^2}\right)\sin\left(k_1 a\right)\cos\left(k_2 b\right), \tag{3.14}$$

and

$$\beta_M=\left(\frac{k_2}{n_2^2\left|k_3\right|^2}-\frac{n_2^2}{k_2\left|\varepsilon_3\right|^2}\right)\cos\left(k_1 a\right)\sin\left(k_2 b\right)+\left(\frac{k_1}{n_1^2\left|k_3\right|^2}-\frac{n_1^2}{k_1\left|\varepsilon_3\right|^2}\right)\sin\left(k_1 a\right)\cos\left(k_2 b\right), \tag{3.15}$$

which also can be substituted in Eqs. (3.8) and (3.9) to find the real and imaginary parts of the Bloch vector for TM modes.

With the results of this section, in the next one we will calculate, numerically, the band structure diagrams for different thickness of metal and for both cases: TE and TM modes.

3.3 Numerical Results: Band Diagrams

As we mentioned before, to plot these band diagrams for off-axis propagation it is necessary to do a scan in all the k_y components and by the same token a full band gap for both polarizations is not expected for oblique incidence in 1D-PC. The explanation is the fact that, oblique propagation has not periodic dielectric regions to coherently scatter the light which originates in this way a band gap [2]. However, it is still possible to generate an omnidirectional reflector for both polarizations for DPCs as well as for the structure under study in this dissertation. In fact, despite this is a very old problem no one has seen an omnidirectional band gap until the work of Joannopoulos' group [3, 4] for a quarter-wave stack of dielectrics. Nevertheless, for not normal incidence, a quarter-wave stack is not the optimal thickness of each material in the crystal but a very good approximation [5].

The truth is, a quarter-wave stack has not a full band gap in the same sense that in a 3D-PC because in this case there are some evanescent modes below the light line $\omega = ck$ and in the former case there is not any mode permitted by the band gap.

The light line is accepted for conventional dielectric photonic crystals but it is not a very good parameter when we are working with mixtures of materials. In particular, if one of the materials present in the mixture has an index of refraction which is a function of frequency. This is precisely the case of metals and, therefore, the stacks that we discuss in the previous chapter. For that

reason, in the case of metallic photonic crystals [6, 7] and metallo-dielectric photonics crystals, to discriminate between evanescent modes and the allowed ones, a special concept should be introduced: Wiener bounds.

Roughly speaking, Wiener bounds are effective dielectric constants for a binary mixture. These effective dielectric constants are different, depending on the polarization of the electromagnetic wave. The limits established by Wiener [8, 9] are absolute in the sense that the region delimited by them, contains all physical realizable quasistatic values of ε for two-phase composites irrespective of microstructure or composition. The minimum screening corresponds with the TE mode, when all boundaries are parallel to this field. Conversely, maximum screening is achievement when all boundaries are parallel to the magnetic field, this is the TM case.

The Wiener bound criteria is no longer valid when the wavelength becomes comparable with the microstructure's composite. There are different forms for establishing the limits in the dielectric response as for example Hashin-Shtrikman limits [10] and others [11-13] but these are more restrictive. Almost all these limits can be reduced to the Wiener bounds under appropriated conditions. Also, Wiener bounds are often used in engineering where they have great importance. In biology and biomedicine as well, there is the problem of a liquid matrix in which a number of different inclusions, such as nanoparticles, appear simultaneously. The same token happens in nanocomposites in the field of Optics.

The crystal, that we proposed, is a ternary composite. Then, a generalization of the Wiener bound limits should be done. Luckily, few years ago, Peiponen and Gornov [14] derived rigorously this generalization. The general form of the Wiener bounds, as presented for the previous authors, is

$$\varepsilon_{\min} = \sum_{i=1}^{m} f_i \varepsilon_i \quad (\mathrm{TE}) \tag{3.16}$$

and

$$\frac{1}{\varepsilon_{\max}} = \sum_{i=1}^{m} \frac{f_i}{\varepsilon_i}, \quad (\mathrm{TM}) \tag{3.17}$$

where f_i is the filling fraction and ε_i is the permittivity of the m-th material that forms the composite.

In our case, we calculated the specific form of the effective dielectric constants for both TE and TM modes. The Wiener bounds in our case are:

$$\varepsilon_{\min} = \frac{1}{L}\left(\varepsilon_1 a + \varepsilon_2 b + \varepsilon_{3R}\delta\right) + i\frac{\varepsilon_{3I}\delta}{L} \quad (\mathrm{TE}) \tag{3.18}$$

and

$$\varepsilon_{\max} = \frac{L\varepsilon_1\varepsilon_2\left(\delta\varepsilon_1\varepsilon_2\varepsilon_{3R} + \left[a\varepsilon_2 + b\varepsilon_1\right]\left|\varepsilon_3\right|^2 + i\delta\varepsilon_1\varepsilon_2\varepsilon_{3I}\right)}{\left(\delta\varepsilon_1\varepsilon_2 + \left[a\varepsilon_2 + b\varepsilon_1\right]\varepsilon_{3R}\right)^2 + \left(a\varepsilon_2 + b\varepsilon_1\right)^2\varepsilon_{3I}^2}, \quad (\mathrm{TM}) \tag{3.19}$$

where all parameters are defined exactly as in chapter two and ε_{3R} and ε_{3I} correspond to the real and imaginary part, respectively, in the Drude model (See Eq. (2.3)).

With these relations we can plot, using the Wiener bounds, the analogy with the light line. Then, in our case

$$k_y = \sqrt{\varepsilon_{eff}\omega^2 - k_x^2} \tag{3.20}$$

where ε_{eff} is the Wiener bound given by Eqs. (3.18) or (3.19) depending on the mode under analysis.

Now, we have all the necessary concepts, to discuss our results, the band diagrams for the TE and TM modes. The parameters used to plot the band diagrams of the MDPC are the same that in chapter two: a = 0.1082 μm, b =

0.2654 μm with indices n_1 = 3.58 and n_2 = 1.46, respectively. The index of the metal is modeled following Drude model whereas the thickness is still a parameter that we will change to study its effect over the band structure.

Fig. 3.2 (a) shows the band diagram when there is not metal in the crystal. In this figure, to the left, we have the TE modes in black color and the light line in gray color. Here we are using the light line to delimit the evanescent modes from the allowed ones, because this is a pure dielectric crystal. TE modes were plotted using the equations that we have derived in the previous section, specifically the Eqs. (3.8) and (3.10) where the substitution of Eqs. (3.3) to (3.7) was required. In analogy, to the right, TM modes are plotted in gray color and the light line in black color. As before, we need Eqs. (3.8) and (3.10) but now using Eqs. (3.11) to (3.15) which correspond to the TM mode.

Also, in the same figure, we can appreciate the existence of very narrow omnidirectional band gaps above the light line. These band gaps are thinner in the TM case than in the TE. However, if we continue extending the band diagram to bigger values of k_y, probably these band gaps would be totally closed for some critical k_y.

In this case, the dispersion relation is a function of the two components of the wave vector: $\omega(\kappa, k_y)$. This means that the band diagrams, shown in Fig. 3.2, are a projection. As we are interested in the oblique propagation, we should plot the k_y component for any value of the Bloch component κ_R but with the restriction that the imaginary part, absorption, will be less than $\kappa_I L/2\pi$ < 0.0001. If the condition of absorption is relaxed, more states would be allowed and the band gaps would be thin. However, the increment in the absorption is not possible because the stack needs at least ten periods (thirty layers dielectric-dielectric-metal) for the formation of full dielectric band gaps.

From Fig. 3.2 (b) to (d), the light line is substituted by Wiener bounds. The motive was explained before, and basically it is the presence of metal in the

crystal. Since the inclusion of very thin metallic layers, δ = 0.0001 μm, we can see how the constrain of the absorption eliminates the TE modes under the corresponding Wiener bound and in the same way TM modes are modified and less modes admitted. For the TM case, there are modes under the Wiener bounds, these modes are evanescent modes. They could be superficial modes coupled or associated to plasmon polariton phenomena.

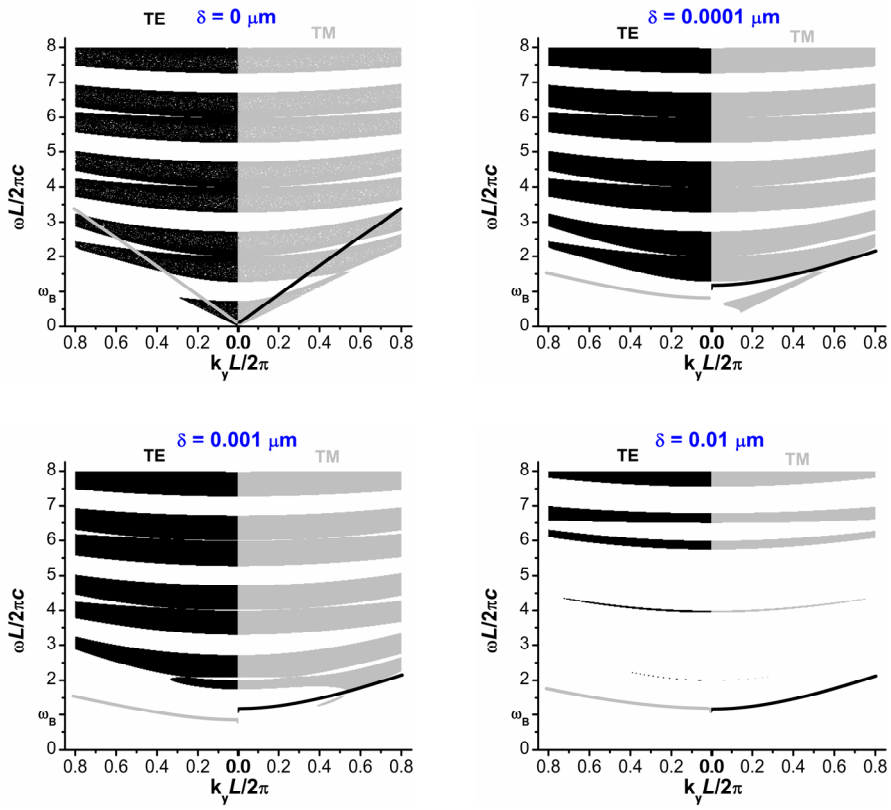

Fig. 3.2. TE and TM modes for different metallic thickness, (a) δ = 0, (b) δ = 0.0001, (c) δ = 0.001 and (d) δ = 0.01 μm. By changing k_y different angles of incidence are selected.

For high frequencies the inclusion of metal is not as dramatic as in the case of low ones. Fig. 3.2 (c) has a bigger band gap at the bottom but there are still some TM modes under the Wiener bounds. So, in this sense there is not an omnidirectional band gap at the bottom because there are superficial

modes in the crystal. But in the last band diagram, when metallic layers have a thickness of δ = 0.01 μm, we clearly have full omnidirectional band gaps inclusive in high frequencies. Comparing this graph with the previous one, we can see an abrupt change in the wide of the band gaps. This is because for this amount of metal (~ 0.01 μm) the validity of band diagrams is near their limit, there is a lot of absorption due to the thickness of the metallic layers.

Finally, it is interesting to mention that the physical realization of omnidirectional band gaps, for a particular combination of materials, in binary stacks is achievable with only nine films, which means four and half periods in total [4] but another authors report nineteen layers [5]. These differences are not surprising because different materials and thickness will require different number of layers. Also, omnidirectional band gaps were reported theoretically, few years ago, in 1D-PC made of one negative-index material and a conventional one [15, 16].

REFERENCES

[1]. A. A. Krokhin and P. Halevi, Phys. Rev. B **53**, 1205 (1996).

[2]. J. D. Joannopoulos, S. G. Johnson, J. N. Winn and R. D. Meade, *Photonic Crystals: Molding the Flow of Light*, Princeton University Press, Singapore, 2008.

[3]. J. N. Winn, Y. Fink, S. Fan and J. D. Joannopoulos, Opt. Lett. **23**, 1573 (1998).

[4]. Y. Fink, J. N. Winn, S. Fan, C. Chen, J. Michel, J. D. Joannopoulos and E. L. Thomas, Science **282,** 1679 (1998).

[5]. D. N. Chigrin, A. V. Lavrinenko, D. A. Yarotsky and S. V. Gaponenko, J. Lightwave Technol. **17**, 2018 (1999).

[6]. M. Bergmair, M. Huber and K. Hingerl, Appl. Phys. Lett. **89**, 081907-1 (2006).

[7]. M. Bergmair and K. Hingerl, J. Opt. A **9**, S339 (2007).

[8]. D. E. Aspnes, Phys. Rev. B **25**, 1358 (1982).

[9]. D. E. Aspnes, Am. J. Phys. **50**, 704 (1982).

[10]. Z. Hashin and S. Shtrikman, J. Appl. Phys. **33**, 3125 (1962).

[11]. D. J. Bergman, Phys. Rev. Lett. **44**, 1285 (1980).

[12]. G. W. Milton, Appl. Phys. Lett. **37**, 300 (1980).

[13]. G. W. Milton, Phys. Rev. Lett. **46**, 542 (1981).

[14]. K-E. Peiponen and E. Gornov, Opt. Lett. **31**, 2202 (2006).

[15]. H. Jiang, H. Chen, H. Li, Y. Zhang and S. Zhu, Appl. Phys. Lett. **83**, 5386 (2003).

[16]. H. Daninthe, S. Foteinopoulou and C. M. Soukoulis, Photon. Nanostruct. **4**, 123 (2006).

CHAPTER FOUR

CONCLUSIONS

Photonic crystals are still a fecund field of research as was shown along this document. Perhaps not in the fundamental physics of this research field by itself but in the combinations of materials and the clever use of the particular features and engineering of band gaps for possible applications as optical devices.

In this dissertation has been shown the existence of a synergic behavior between a metallic photonic crystal and the dielectric one giving origin to a ternary material, named metallo-dielectric photonic crystal, with both desire characteristics of the original structures and new ones owned by the MDPC due to its geometric features and proportions when metal is combined with the dielectric crystal.

In the ternary structure, the original band gaps of the dielectric crystal are conserved and the width of them incremented by the presence of metal. Also, the band gap at the bottom, characteristic of metallic photonic crystals, is present. This band gap is mainly due to the absorption of metal for frequencies below the plasma frequency. Moreover, new band gaps appear in the metallo-dielectric photonic crystal additional to the ones mentioned before.

These new band gaps are very thing and are structural ones, attributed to the periodicity of the stack and not just to the absorption, in contrast with the band gap which exists before the plasma frequency. The thin metallic band gaps are situated exactly between two adjacent dielectric band gaps when the metallic layers are thin. We use transmittance to verify the existence of the new band gaps and it agrees very well for low thickness of metal. However, when the thickness of the metallic layers is bigger than 0.01 μm, band gaps disagree with the transmittance. This means that band diagrams are no longer valid for high absorption given origin to flat bands.

Therefore, we compared two different approaches, transmittance and dispersion relation. The first one is always valid for the amounts of metal studied in the metallo-dielectric photonic crystal and should be calculated for a specific number of layers, that can be big enough but finite after all. Whereas band structure is understand as the modes allowed in an infinite structure where commonly losses are not considered. Thus, band gaps and stop gaps coincide in the case of a pure dielectric photonic crystal.

In contrast, as a result of the introduction of metal, and therefore absorption, our results show that for ultra thin and thin metallic layers band gaps and stops gaps coincide. The last one guarantees us that, effectively a narrow band gap exists. Nevertheless, when metal is thick our results suggest that band diagrams cannot be trusted and transmittance should be considered as the real behavior of the frequencies inside the structure.

On the other hand, two forms for finding the Bloch wave numbers in the dispersion relation were discussed. The first one, is the traditional way in literature, consists in solving the dispersion relation numerically with iterative techniques. This method requires long times of computing and in our case shows problems with the convergence of the values.

The second approach, that we proposed, is an analytical procedure, consisting in calculate the inverse function of a cosine for complex numbers. This method is possible because there is a specific real and imaginary part in the dispersion relation since the beginning due to the presence of the metal. Thus, the Bloch wave numbers can be calculated just evaluating the analytical expressions, Eqs. (2.16) and (2.17), which we derived in chapter two. Using these equations there are not problems either with the time of computing or the convergence of the values. In contrast, the dispersion relation of a pure dielectric crystal is only complex for a range of values where the band gap is localized and cannot be separated in general in real and imaginary part for all values.

In chapter three, we extended our analytical results for normal incidence to the case of oblique incidence. This means, that we found the dispersion relation for transversal electric and transversal magnetic modes. After that, band diagrams for TE and TM modes were plotted for different amount of metal.

A remarkable result for oblique incidence is the existence of omnidirectional band gaps, which in the same manner that for normal incidence, they are present not only at low frequencies but also after the plasma frequency.

Therefore, the structure that we proposed and studied in this research has possible applications as an optical device in two different ways. For normal incidence we can use it as a very thin band pass filter and the opposite happen for oblique incidence. In that case the MDPC can be used as very narrow selector for only a narrow width of frequencies.

Future Work

The line of future research that we proposed is an extension of the metallo-dielectric photonic crystal, analyzed previously, to the two dimensional case.

With the experience developed in the 1D crystal is possible to calculate the band diagrams for a 2D crystal with a closed dispersion relation, using transfer matrix method in two dimensions.

Such structure is a net of infinite long rods with square cross section. For this crystal three or four different materials can be used in its construction. A top view of the unit cell is shown in Fig. 4.1 (a). Of course, this crystal only can be quarter-wave in some directions but not in all them.

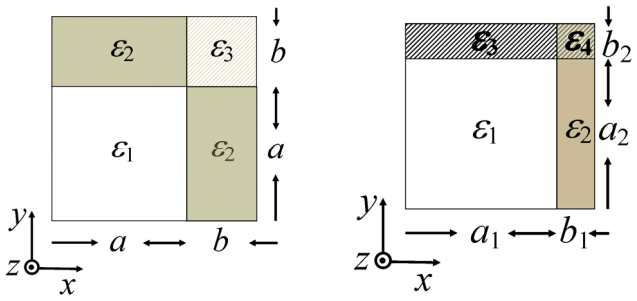

Fig. 4.1. (a) Top view of a unit cell of a two dimensional quarter-wave like crystal. (b) Top view of a unit cell for a metallo-dielectric photonic crystal. ε_1 and ε_2 are dielectrics while ε_3 and ε_4 are metals.

After the study and understanding of the dielectric case, several possibilities can be explored. For example, metal can be introduced to the crystal as one of the thin rods which form the unit cell (see Fig. 4.1 (b)) or just conserving the dielectric unit cell of Fig. 4.1 (a) a metallic shell can be introduced coating in this way the dielectric structure. We believed that the band structure of the 2D dielectric photonic crystal will be strongly modified, perhaps generating a full band gap not only at low frequencies but also at high ones in the same way that the 1D case.

APPENDIX

TRANSFER MATRIX METHOD

In this section the transfer matrix method (TMM) shall be described in detail. However, the procedure shown here is not exactly the standard TMM but a modification that mix the usual way in Quantum Mechanics (QM) and the procedure followed in Optics [1].

There are mayor differences between these fields of physics. In QM the wave packed is associated to a free particle, which is material but the atomic dimensions. This wave packed describes the state of the systems through a wave function ψ and the square of its modulus is interpreted as a probability density for a particle in the state ψ. The wave function ψ has the same mathematical structure of a traveling wave of the exponential kind but not the same interpretation as was mentioned before.

In contrast, Physical Optics describes electric and magnetic fields as a superposition of plane waves traveling in opposite directions. The mathematical representation is exactly the same that the one used in QM. However, the physical interpretation here is that the coefficients of the exponential functions (the real part) are the amplitudes of the fields traveling in a particular direction, and the square of its modulus is interpreted as intensity of the field directly related to the energy of the same.

In addition, when QM boundary conditions are invoked ψ and $d\psi/dx$ must be continuous. The first one condition, the wave function continuous, has physical meaning because a physical phenomena change gradually except possibly in a phase transition. So, the function that describes it, must be continuous. However, the continuity in the derivate of the wave function is a stronger mathematical assumption that is made principally just to justify the condition of normalization of the wave function. Whereas, in general, in Electromagnetic Theory both conditions, the continuity in the plane wave in the boundaries, have physical meaning and the electric field and its derivative are continuous not by a mathematical assumption but because the Maxwell equations: the electric and magnetic field satisfy each one a different continuity condition that results in a natural manner, after algebraic manipulation, in the continuity of the electric field and its derivative and also in the continuity of the magnetic field and its own derivative.

Nonetheless, the differences in the methodology that we mention at the beginning are not located in the physics itself but in the mathematical procedure. The classical procedure defines an extra matrix, named propagation matrix, with the information of the change of phase through a layer. This additional matrix allowed us to calculate transmittance in a specific interface along the stack. Nevertheless, we are not interested in the transmittance in an explicit point inside the crystal but at the end of a particular full unit cell. Thus, in our methodology, the information of the phase is explicitly included in the exponential function that describes the propagating wave plane.

The transfer matrix methodology will be applied to the well-known dielectric-dielectric stack which is shown in Fig. A.1. It is made of two different dielectrics with indices n_1 and n_2, the thickness of each layer is a and b respectively. The length of a unit cell is $L = a + b$, i.e., a period.

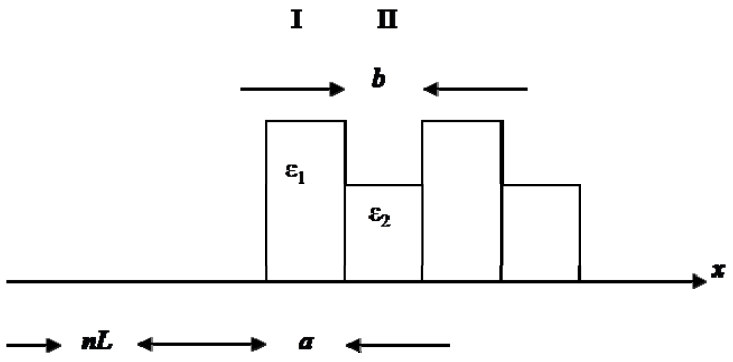

Fig. A.1. Stack of two different dielectrics with indices n_1 and n_2.

In this case, the general electric field could be written as

$$E = E_z\left(x\right)e^{i(\omega t - k_x x)} \tag{A1}$$

where $E_z(x)$ is the field perpendicular to this page and changing with the periodic direction, ω is the frequency of the field, t the time, k_x the wave number in the direction of propagation and y is perpendicular to the periodicity in a right-handed system.

For a homogeneous layer we can consider the $E_z(x)$ field as a superposition of two waves, one incident and the other one reflected. First the (n+1)-th unit cell will be considered, in this cell the electric field in the region I, for normal incidence, is

$$E_I\left(x\right) = A_n e^{-ik_1(x-nL)} + B_n e^{ik_1(x-nL)} \qquad \left(nL < x < nL + a\right) \tag{A2}$$

where A_n and B_n are the amplitudes of the fields traveling to the left and to the right respectively. The wave number in the x direction is k_1. In the same way the region II has:

$$E_{II}\left(x\right) = C_n e^{-ik_2(x-nL-a)} + D_n e^{ik_2(x-nL-a)} \qquad \left(nL + a < x < \left(n+1\right)L\right) \tag{A3}$$

as before C_n and D_n are the amplitudes of the fields traveling to the left and to the right, respectively, in this region. Here the wave number in the x direction is k_2.

The wave number is defined in the usual way

$$k_i = \frac{\omega}{c} n_i \quad (i = 1, 2). \tag{A4}$$

This is because the index of refraction has the profile

$$n(x) = \begin{cases} n_1, & nL \le x < nL + a \\ n_2, & nL + a \le x < (n+1)L \end{cases} \tag{A5}$$

also it satisfies the relation of periodicity

$$n(x) = n(x + L). \tag{A6}$$

The following is to invoke the continuity conditions in the electric and magnetic fields, in agreement with the Maxwell's equations,

$$\begin{aligned} E_I(nL + a) &= E_{II}(nL + a) \\ H_{yI}(nL + a) &= H_{yII}(nL + a). \end{aligned} \tag{A7}$$

So, for the electric field in the boundary between region I and II, yields

$$A_n e^{-ik_1(nL+a-nL)} + B_n e^{ik_1(nL+a-nL)} = C_n e^{-ik_2(nL+a-nL-a)} + D_n e^{ik_2(nL+a-nL-a)}. \tag{A8}$$

Or simplifying

$$A_n e^{-ik_1 a} + B_n e^{ik_1 a} = C_n + D_n. \tag{A9}$$

On the other hand, for the magnetic field the y component H_y is

$$H_y(x) = \frac{1}{i\omega\mu} \frac{\partial E_z(x)}{\partial x} \tag{A10}$$

where μ is the magnetic permeability which in our case and for both materials is $\mu \approx 1$ due to the materials are not magnetic. Thus, as before, in the same interface due to the continuity condition,

$$-ik_1 A_n e^{-ik_1 a} + ik_1 B_n e^{ik_1 a} = -ik_2 C_n + ik_2 D_n. \tag{A11}$$

Next Eqs. (A9) and (A11) are rewritten in the matrix formalism:

$$M_{AB}^{12}\begin{pmatrix} A_n \\ B_n \end{pmatrix} = M_{CD}^{12}\begin{pmatrix} C_n \\ D_n \end{pmatrix} \tag{A12}$$

where

$$M_{AB}^{12} = \begin{pmatrix} e^{-ik_1 a} & e^{ik_1 a} \\ -ik_1 e^{-ik_1 a} & ik_1 e^{ik_1 a} \end{pmatrix} \tag{A13}$$

and

$$M_{CD}^{12} = \begin{pmatrix} 1 & 1 \\ -ik_2 & ik_2 \end{pmatrix}. \tag{A14}$$

Here the superscript means from interface 1 to 2 and the subscript the coefficients of the field's amplitudes. In this manner Eq. (A12) can be written as

$$\begin{pmatrix} C_n \\ D_n \end{pmatrix} = \left(M_{CD}^{12}\right)^{-1} M_{AB}^{12}\begin{pmatrix} A_n \\ B_n \end{pmatrix}. \tag{A15}$$

Now the same is done with the interface between region II and I, evaluating the fields after a full period, in the matrix representation

$$\begin{pmatrix} A_{n+1} \\ B_{n+1} \end{pmatrix} = \left(M_{AB}^{21}\right)^{-1} M_{CD}^{21}\begin{pmatrix} C_n \\ D_n \end{pmatrix} \tag{A16}$$

where

$$M_{AB}^{21} = \begin{pmatrix} 1 & 1 \\ -ik_1 & ik_1 \end{pmatrix} \tag{A17}$$

and

$$M_{CD}^{21} = \begin{pmatrix} e^{-ik_2 b} & e^{ik_2 b} \\ -ik_2 e^{-ik_2 b} & ik_2 e^{ik_2 b} \end{pmatrix}. \tag{A18}$$

Substituting (A15) into Eq. (A16), it is obtained

$$\begin{pmatrix} A_{n+1} \\ B_{n+1} \end{pmatrix} = M_T \begin{pmatrix} A_n \\ B_n \end{pmatrix} \tag{A19}$$

where the transfer matrix is

$$M_T = \left(M_{AB}^{21}\right)^{-1} M_{CD}^{21} \left(M_{CD}^{12}\right)^{-1} M_{AB}^{12}. \tag{A20}$$

Finally, it is simplified, after some algebraic manipulation, as

$$M_T = \begin{pmatrix} \left[\cos(k_2 b) - \frac{i\left(k_1^2 + k_2^2\right)}{2k_1 k_2}\sin(k_2 b)\right] e^{-ik_1 a} & \frac{i}{2}\frac{k_1^2 - k_2^2}{k_1 k_2}\sin(k_2 b) e^{ik_1 a} \\ -\frac{i}{2}\frac{k_1^2 - k_2^2}{k_1 k_2}\sin(k_2 b) e^{-ik_1 a} & \left[\cos(k_2 b) + \frac{i\left(k_1^2 + k_2^2\right)}{2k_1 k_2}\sin(k_2 b)\right] e^{ik_1 a} \end{pmatrix}. \tag{A21}$$

The transfer matrix M_T propagates the electric field from one cell to another one, or the number of cells needed just taking as many potencies of itself as unit cells you want to propagate the field. Through M_T two important functions, directly related to the frequency and indices of refraction, can be calculated and that, in some sense, has similar physical information of the structure under analysis: the transmittance and the dispersion relation.

Due to the features of the transfer matrix it is possible to calculate the transmittance of the system by [2]

$$T_n = \frac{1}{\left|M_{22}\right|^2}, \tag{A22}$$

M_{22} is the element of the transfer matrix since the first layer to the n unit cell. Transmittance can be calculated for any number of layers but here the expression given is just applicable to a number of integer unit cells. As well, the reflectance can be found using M_T as follows

$$R_n = \left|\frac{M_{21}}{M_{22}}\right|^2, \tag{A23}$$

where M_{21} also refers to the corresponding element of the transfer matrix for n unit cells. In this manner, for dielectrics with no absorption present, the next relation is satisfied

$$T + R = 1. \tag{A24}$$

There is another way to calculate the transmittance and reflectance. This procedure takes account of all the reflections and refractions inside the structure in the different interfaces in the same fashion that in a Fabry-Perot interferometer. The explicit coefficients given by Fresnel's formulas are summed for the rays reflected and transmitted in each interface, using a formula to sum all the terms in the series, arriving in this manner to the Airy's formulas [1].

The last procedure is transparent in the TMM in the sense that all the contributions of the reflections and refractions are being summed through the process of the matrix product and as has been seen before the final transfer matrix, until the unit cell or layer wished, has the information of the total of the energy transmitted and reflected with respect to the original input.

The dispersion relation can be calculated through

$$\cos\left(\kappa L\right) = \frac{1}{2} Tr\left\{M_T\right\} \tag{A25}$$

where κ is the Bloch wave number, L is the length of a period and Tr denotes the operation of trace over the transfer matrix. After the substitution of the

elements of the transfer matrix and doing all the algebraic procedure the dispersion relation is given by

$$\cos(\kappa L) = \cos(k_1 a)\cos(k_2 b) - \frac{k_1^2 + k_2^2}{2k_1 k_2}\sin(k_1 a)\sin(k_2 b). \qquad \text{(A26)}$$

The plot of the dispersion relation contains all the information about the frequencies that can propagate through the crystal and it is called band diagram or band structure in analogy to the energy band diagrams for electrons in Solid State Physics [3].

REFERENCES

[1]. P. Yeh, *Optical Waves in Layered Media*, Wiley & Sons, New Jersey, 2005.

[2]. E. Merzbacher, *Quantum Mechanics*, Wiley & Sons, New York, 1998.

[3]. C. Kittel, *Introduction to Solid State Physics*, Wiley, New York, 1996.